

Accepted Manuscript

Two Improved Multiband Structured Subband Adaptive Filter Algorithms with Reduced Computational Complexity

Mohammad Shams Esfand Abadi, John Håkon Husøy,
Mohammad Javad Ahmadi

PII: S0165-1684(18)30262-7
DOI: <https://doi.org/10.1016/j.sigpro.2018.08.001>
Reference: SIGPRO 6893



To appear in: *Signal Processing*

Received date: 25 January 2018
Revised date: 31 July 2018
Accepted date: 1 August 2018

Please cite this article as: Mohammad Shams Esfand Abadi, John Håkon Husøy, Mohammad Javad Ahmadi, Two Improved Multiband Structured Subband Adaptive Filter Algorithms with Reduced Computational Complexity, *Signal Processing* (2018), doi: <https://doi.org/10.1016/j.sigpro.2018.08.001>

This is a PDF file of an unedited manuscript that has been accepted for publication. As a service to our customers we are providing this early version of the manuscript. The manuscript will undergo copyediting, typesetting, and review of the resulting proof before it is published in its final form. Please note that during the production process errors may be discovered which could affect the content, and all legal disclaimers that apply to the journal pertain.

HIGHLIGHTS

- The improved multiband structured subband adaptive filter (IMSAF) utilizes the input regressors at each subband to speed up the convergence rate of MSFA. When the number of input regressors is increased, the convergence rate of the IMSAF algorithm improves at the cost of increased complexity. The current study introduces two new IMSAF algorithms with low computational complexity feature. In the first algorithm, a subset of input regressors at each subband is optimally picked out during the adaptation. In the second approach, the number of selected input regressors is dynamically changed at each subband for every iteration. The introduced algorithms are called selective regressor IMSAF (SR-IMSAF) and dynamic selective regressor IMSAF (DSR-IMSAF). The SR-IMSAF and DSR-IMSAF are shown to be capable of outperforming the full-update IMSAF while the computational complexity is kept low. In the following, the general update equation to establishment of the family of IMSAF algorithms is presented. Accordingly, the mean-square performance analysis of the algorithms is studied in a unified way and the general theoretical expressions for transient, steady-state, and the stability bounds for IMSAF, SR-IMSAF, and DSR-IMSAF are derived. The good performance of the introduced algorithms and the validity of the derived theoretical relations are justified by presenting various experimental results.
- We divided the contribution of the paper into the following four sections: A. Establishment of the Family of IMSAF Algorithms The SR-IMSAF and the DSR-IMSAF algorithms are established. These algorithms have the following features: 1) SR-IMSAF algorithm: The SR strategy is applied in IMSAF algorithm. In this algorithm, the input regressors are optimally selected at each subband during the adaptation. The SR-IMSAF has close performance to the conventional IMSAF while the computational complexity is kept low. 2) DSR-IMSAF algorithm: The DSR approach is extended to IMSAF and DSR-IMSAF is proposed. In DSRIMSAF, the number of selected input regressors is dynamically changed at each subband for every iteration. This algorithm has a fast convergence speed and a small steady-state error compared to the conventional IMSAF. In addition, the DSR-IMSAF retains a low overall computational complexity.
- B. General Update Equation We extend the general update equation in [20] to establishment of the family of IMSAF algorithms. The IMSAF, SR-IMSAF, and DSR-IMSAF can be derived from the generic update equation. By substituting the parameters and the matrices in this equation, various IMSAF algorithms will be established. Also, this representation will be useful to analyze the mean-square performance of the family of IMSAF algorithms in a unified way.
- C. Mean-Square Performance Analysis The theoretical transient and steady-state analyses and the stability bounds of the proposed algorithms will be studied in a unified way. 1) Transient analysis: The mean-square performance of the family of IMSAF algorithms is analyzed in a unified way and the transient behaviors are studied. 2) Steady-state analysis: The generic closed form expressions for steady-state mean-square error (MSE) and mean-square coefficient deviation (MSD) of IMSAF, SR-IMSAF, and DSR-IMSAF are derived.

3) Stability bounds analysis: The theoretical stability bounds of IMSAF, SR-IMSAF, and DSR-IMSAF are extracted.

- D. Simulation Results 1) The performance of the family of IMSAF algorithms is compared in convergence speed, steady-state error and computational complexity features. 2) The validity of the theoretical relations for transient and steady-state performances and the stability bounds is verified.

ACCEPTED MANUSCRIPT

Two Improved Multiband Structured Subband Adaptive Filter Algorithms with Reduced Computational Complexity

Mohammad Shams Esfand Abadi, John Håkon Husøy, and Mohammad Javad Ahmadi

Abstract

The improved multiband structured subband adaptive filter (IMSAF) utilizes the input regressors at each subband to speed up the convergence rate of MSAF. When the number of input regressors is increased, the convergence rate of the IMSAF algorithm improves at the cost of increased complexity. The current study introduces two new IMSAF algorithms with low computational complexity feature. In the first algorithm, a subset of input regressors at each subband is optimally picked out during the adaptation. In the second approach, the number of selected input regressors is dynamically changed at each subband for every iteration. The introduced algorithms are called selective regressor IMSAF (SR-IMSAF) and dynamic selective regressor IMSAF (DSR-IMSAF). The SR-IMSAF and DSR-IMSAF are shown to be capable of outperforming the full-update IMSAF while the computational complexity is kept low. In the following, the general update equation to establishment of the family of IMSAF algorithms is presented. Accordingly, the mean-square performance analysis of the algorithms is studied in a unified way and the general theoretical expressions for transient, steady-state, and the stability bounds for IMSAF, SR-IMSAF, and DSR-IMSAF are derived. The good performance of the introduced algorithms and the validity of the derived theoretical relations are justified by presenting various experimental results.

Index Terms

Improved multiband structured subband adaptive filter, mean-square performance, selective regressors, convergence rate, computational complexity

I. INTRODUCTION

Adaptive filters are applied in many applications such as system identification, channel equalization, signal prediction, and noise cancellation [1], [2], [3]. In these applications, the generated signals are processed to identify the impulse response of the unknown system. This objective is successfully achieved by using adaptive filters rather

The revised manuscript submitted on July 31, 2018.

Mohammad Shams Esfand Abadi and Mohammad Javad Ahmadi are with the Faculty of Electrical Engineering, Shahid Rajaee Teacher Training University, P.O.Box: 16785-163, Tehran, Iran, Email: mshams@srttu.edu. John Håkon Husøy is with the Department of Electrical Engineering and Computer Science, Faculty of Science and Engineering, University of Stavanger, Norway, Email: john.h.husoy@uis.no

than conventional digital filters. The adaptive filters utilize a recursive algorithm to design itself. The algorithm updates the filter coefficients through successive iterations and finally converges to the optimal Wiener-Hopf solution. The performance of an adaptive filtering algorithm is evaluated by the rate of convergence, misadjustment, and computational complexity features. The conventional LMS adaptive filter algorithm has the advantage of being very simple; it is easy to implement; and it has a very low computational complexity. However, when the input signal is highly colored, the LMS convergence slows down [3], [4]. To improve the convergence behavior of the LMS, various adaptive algorithms such as affine projection algorithm (APA) and multiband-structured subband adaptive filter (MSAF) were proposed [5], [6]. To increase the convergence speed of MSAF, the variable step-size MSAF (VSS-MSAF) was introduced [7]. Due to VSS, the computational complexity in VSS-MSAF increases.

The APA is one of the important family of adaptive filter algorithm. This algorithm uses the recent input regressors in filter coefficients adaptation. Since the interplay between the computational complexity and the performance of adaptive signal processing systems is important, several types of affine projection algorithms such as selective partial update APA (SPU-APA) have been proposed [8]. Also, in selective regressor APA (SR-APA), a subset of recent regressors at every iteration is optimally selected and utilized in APA [9]. The dynamic selection (DS) of recent regressors during the filter coefficients adaptation was suggested in [10]. It has been shown that the SR-APA and DS-APA have better performance than APA [9], [10]. Furthermore, by combining SPU and SR approaches, the SPU-SR-APA was introduced [11].

Another important classes of adaptive filters are subband adaptive filter (SAF) algorithms [12], [13]. Lee and Gan [6] developed the MSAF based on a constrained optimization problem. In comparison with NLMS, the MSAF algorithm has better convergence speed. The same as APA, to reduce the computational complexity of MSAF, different methods were proposed. In [14], the selective partial update MSAF (SPU-MSAF) algorithm was presented where the filter coefficients are partially updated rather than the entire filter at every adaptation. In [15], the dynamic selection of MSAF (DS-MSAF) algorithm was introduced. In this algorithm, the number of subbands was dynamically selected during each iteration. The FS-MSAF was also proposed in [16]. In this algorithm, a subset of subbands was selected during the adaptation.

To increase the convergence speed of MSAF, the improved MSAF (IMSAF) was developed [17], [18], [19]. This algorithm utilizes the input regressors at each subband during the adaptation; however, the computational complexity of this algorithm is high. This paper proposes a solution to reduce the computational load of the IMSAF algorithm. In the first approach, the SR strategy is extended to IMSAF algorithm. In SR-IMSAF, the input regressors at each subband are optimally selected at each iteration. In the second method, the number of selected input regressors is dynamically changed at each subband for every adaptation. In the following, the general update equation for the family of IMSAF algorithms is proposed. Based on this, the general mean-square performance analysis is introduced and the theoretical relations for transient and steady-state performances are derived.

We divided the contribution of the paper into the following four sections:

A. Establishment of the Family of IMSAF Algorithms

The SR-IMSAF and the DSR-IMSAF algorithms are established. These algorithms have the following features:

- 1) SR-IMSAF algorithm: The SR strategy is applied in IMSAF algorithm. In this algorithm, the input regressors are optimally selected at each subband during the adaptation. The SR-IMSAF has close performance to the conventional IMSAF while the computational complexity is kept low.
- 2) DSR-IMSAF algorithm: The DSR approach is extended to IMSAF and DSR-IMSAF is proposed. In DSR-IMSAF, the number of selected input regressors is dynamically changed at each subband for every iteration. This algorithm has a fast convergence speed and a small steady-state error compared to the conventional IMSAF. In addition, the DSR-IMSAF retains a low overall computational complexity.

B. General Update Equation

We extend the general update equation in [20] to establishment of the family of IMSAF algorithms. The IMSAF, SR-IMSAF, and DSR-IMSAF can be derived from the generic update equation. By substituting the parameters and the matrices in this equation, various IMSAF algorithms will be established. Also, this representation will be useful to analyze the mean-square performance of the family of IMSAF algorithms in a unified way.

C. Mean-Square Performance Analysis

The theoretical transient and steady-state analyses and the stability bounds of the proposed algorithms will be studied in a unified way.

- 1) Transient analysis: The mean-square performance of the family of IMSAF algorithms is analyzed in a unified way and the transient behaviors are studied.
- 2) Steady-state analysis: The generic closed form expressions for steady-state mean-square error (MSE) and mean-square coefficient deviation (MSD) of IMSAF, SR-IMSAF, and DSR-IMSAF are derived.
- 3) Stability bounds analysis: The theoretical stability bounds of IMSAF, SR-IMSAF, and DSR-IMSAF are extracted.

D. Simulation Results

- 1) The performance of the family of IMSAF algorithms is compared in convergence speed, steady-state error and computational complexity features.
- 2) The validity of the theoretical relations for transient and steady-state performances and the stability bounds is verified.

This paper is organized as follows. In Section II, the IMSAF algorithm is reviewed. Section III presents the SR-IMSAF algorithms. The DSR-IMSAF is established in Section IV. The general update equation for the IMSAF algorithm is introduced in Section V. The extension of this framework to SR-IMSAF and DSR-IMSAF is given in

Section VI. The theoretical stability bounds of the introduced algorithms are presented in Section VII. The general mean-square performance analysis of these algorithms is studied in Section VIII. The computational complexity of the proposed algorithms is studied in Section IX. Finally, before concluding the paper, we demonstrate the usefulness of the proposed algorithms by presenting several experimental results.

Throughout the paper, the following notations are used:

$ \cdot $	Norm of a scalar.
$\ \cdot\ ^2$	Squared Euclidean norm of a vector.
$\text{Tr}(\cdot)$	Trace of a matrix.
$(\cdot)^T$	Transpose of a vector or a matrix.
$E\{\cdot\}$	Expectation operator.
$\text{diag}\{\dots\}$	Creates a diagonal matrix with the elements in $\{\dots\}$.
$\text{bdiag}\{\dots\}$	Creates a block diagonal matrix with the matrices in $\{\dots\}$.
$\ \mathbf{t}\ _{\Sigma}^2$	Σ -Weighted Euclidean norm of a column vector \mathbf{t} defined as $\mathbf{t}^T \Sigma \mathbf{t}$.
$\text{vec}(\mathbf{T})$	Creates an $M^2 \times 1$ column vector \mathbf{t} through stacking the columns of the $M \times M$ matrix \mathbf{T} .
$\text{vec}(\mathbf{t})$	Creates an $M \times M$ matrix \mathbf{T} from the $M^2 \times 1$ column vector \mathbf{t} .

II. BACKGROUND ON IMSAF

Consider a linear data model for $d(n)$:

$$d(n) = \mathbf{x}^T(n) \mathbf{w}^o + v(n), \quad (1)$$

where \mathbf{w}^o is an unknown M -dimensional vector that we aim to estimate, $v(n)$ is the measurement noise with variance σ_v^2 , and $\mathbf{x}(n) = [x(n), x(n-1), \dots, x(n-M+1)]^T$ denotes an M -dimensional input (regressor) vector. It is assumed that $v(n)$ is zero mean, white, Gaussian, and independent of $\mathbf{x}(n)$. Fig. 1 shows the structure of the MSAF [6]. In this figure, $\mathbf{f}_0, \mathbf{f}_1, \dots, \mathbf{f}_{N-1}$ and $\mathbf{g}_0, \mathbf{g}_1, \dots, \mathbf{g}_{N-1}$, are analysis and synthesis filter unit pulse responses of an N channel orthogonal perfect reconstruction critically sampled filter bank system. $x_i(n)$ and $d_i(n)$ are nondecimated subband signals. It is important to note that n refers to the index of original sequences and k denotes the index of decimated sequences ($k = \text{floor}(n/N)$). The decimated output signal is defined as $y_{i,D}(k) = \mathbf{x}_i^T(k) \mathbf{w}(k)$ where $\mathbf{x}_i(k) = [x_i(kN), x_i(kN-1), \dots, x_i(kN-M+1)]^T$ and $\mathbf{w}(k) = [w_0(k), w_1(k), \dots, w_{M-1}(k)]^T$. Also, the decimated subband error signal is expressed as $e_{i,D}(k) = d_{i,D}(k) - \mathbf{x}_i^T(k) \mathbf{w}(k)$. The filter update equation for MSAF can be stated as

$$\mathbf{w}(k+1) = \mathbf{w}(k) + \mu \sum_{i=0}^{N-1} \frac{\mathbf{x}_i(k)}{\|\mathbf{x}_i(k)\|^2} e_{i,D}(k), \quad (2)$$

where μ is the step-size. The IMSAF minimizes the following cost function

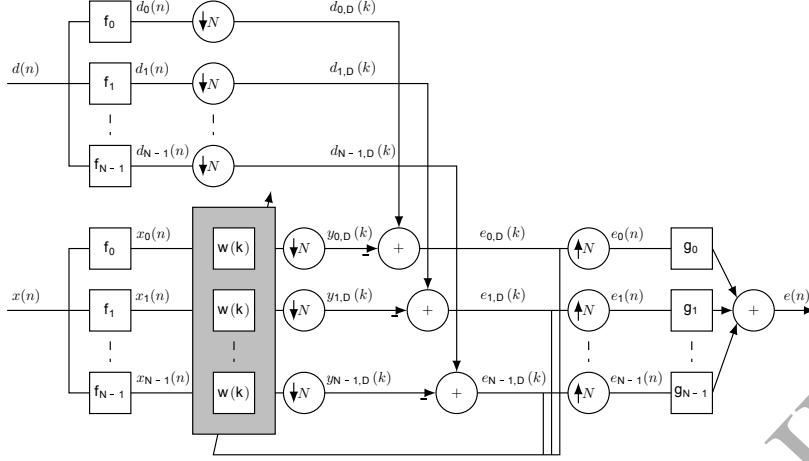


Fig. 1. Structure of the MSAF algorithm.

$$\min \|\mathbf{w}(k+1) - \mathbf{w}(k)\|^2, \quad (3)$$

subject to

$$\mathbf{d}_{i,D}(k) = \mathbf{X}_i^T(k) \mathbf{w}(k+1), \quad (4)$$

where

$$\mathbf{X}_i(k) = [\mathbf{x}_i(k), \mathbf{x}_i(k-1), \dots, \mathbf{x}_i(k-P+1)], \quad (5)$$

and

$$\mathbf{d}_{i,D}(k) = [d_{i,D}(k), \dots, d_{i,D}(k-P+1)]^T. \quad (6)$$

The parameter P is the number of recent regressors in subbands. Therefore, the IMSAF algorithm is derived from the solution of the following constraint minimization problem:

$$\Theta(k) = \|\mathbf{w}(k+1) - \mathbf{w}(k)\|^2 + \sum_{i=0}^{N-1} \Lambda_i [\mathbf{d}_{i,D}(k) - \mathbf{X}_i^T(k) \mathbf{w}(k+1)], \quad (7)$$

where $\Lambda_i = [\lambda_{i,1}, \lambda_{i,1}, \dots, \lambda_{i,P}]$ is the Lagrange multipliers vector with length P . Using $\frac{\partial \Theta(k)}{\partial \mathbf{w}(k+1)} = 0$ and $\frac{\partial \Theta(k)}{\partial \Lambda_i} = 0$, we get

$$\mathbf{w}(k+1) = \mathbf{w}(k) + \frac{1}{2} \sum_{i=0}^{N-1} \mathbf{X}_i(k) \Lambda_i^T, \quad (8)$$

where

$$\Lambda_i^T = 2[\mathbf{X}_i^T(k) \mathbf{X}_i(k)]^{-1} \mathbf{e}_{i,D}(k), \quad (9)$$

and

$$\mathbf{e}_{i,D}(k) = \mathbf{d}_{i,D}(k) - \mathbf{X}_i^T(k) \mathbf{w}(k). \quad (10)$$

Therefore, the update equation for IMSAF becomes

$$\mathbf{w}(k+1) = \mathbf{w}(k) + \mu \sum_{i=0}^{N-1} \mathbf{X}_i(k) [\mathbf{X}_i^T(k) \mathbf{X}_i(k)]^{-1} \mathbf{e}_{i,D}(k). \quad (11)$$

To take care of the possibility that $[\mathbf{X}_i^T(k) \mathbf{X}_i(k)]$ may be close to singular, it is replaced by $[\epsilon \mathbf{I} + \mathbf{X}_i^T(k) \mathbf{X}_i(k)]$, where ϵ is the regularization parameter. Note that for $P = 1$, the conventional MSFA is established.

III. THE SR-IMSAF ALGORITHM

To reduce the computational complexity of IMSAF, the SR-IMSAF is proposed. In SR-IMSAF, a subset of the input regressors at each subband is optimally selected for every adaptation. Let $J_S = \{j_1, j_2, \dots, j_S\}$ denote a S -subset (subset with S members) of the $\{0, 1, \dots, P-1\}$. The SR-IMSAF minimizes (3) subject to $\mathbf{d}_{i,D,J_S}(k) = \mathbf{X}_{i,J_S}^T(k) \mathbf{w}(k+1)$, where

$$\mathbf{d}_{i,D,J_S}(k) = [d_{i,D}(k-j_1), \dots, d_{i,D}(k-j_S)]^T, \quad (12)$$

and

$$\mathbf{X}_{i,J_S}(k) = [\mathbf{x}_i(k-j_1), \mathbf{x}_i(k-j_2), \dots, \mathbf{x}_i(k-j_S)]. \quad (13)$$

Therefore, the cost function for the SR-IMSAF is given by

$$\Theta_{J_S}(k) = \|\mathbf{w}(k+1) - \mathbf{w}(k)\|^2 + \sum_{i=0}^{N-1} \Lambda_i [\mathbf{d}_{i,D,J_S}(k) - \mathbf{X}_{i,J_S}^T(k) \mathbf{w}(k+1)], \quad (14)$$

where $\Lambda_i = [\lambda_{i,1}, \lambda_{i,2}, \dots, \lambda_{i,S}]$ indicates the Lagrange multipliers vector with length S . Following the same approach as IMSAF, we get

$$\mathbf{w}(k+1) = \mathbf{w}(k) + \frac{1}{2} \sum_{i=0}^{N-1} \mathbf{X}_{i,J_S}(k) \Lambda_i^T, \quad (15)$$

where $\Lambda_i^T = 2[\mathbf{X}_{i,J_S}^T(k) \mathbf{X}_{i,J_S}(k)]^{-1} \mathbf{e}_{i,D,J_S}(k)$, and

$$\mathbf{e}_{i,D,J_S}(k) = \mathbf{d}_{i,D,J_S}(k) - \mathbf{X}_{i,J_S}^T(k) \mathbf{w}(k). \quad (16)$$

Then, the update equation for SR-IMSAF is established as

$$\mathbf{w}(k+1) = \mathbf{w}(k) + \mu \sum_{i=0}^{N-1} \mathbf{X}_{i,J_S}(k) [\epsilon \mathbf{I} + \mathbf{X}_{i,J_S}^T(k) \mathbf{X}_{i,J_S}(k)]^{-1} \mathbf{e}_{i,D,J_S}(k). \quad (17)$$

We should select the regressors which make $\Theta_{J_S}(k)$ as close as possible to $\Theta(k)$. Suppose that the amount of filter coefficients update is small. Therefore, the posteriori errors $\mathbf{d}_{i,D}(k) - \mathbf{X}_i^T(k) \mathbf{w}(k+1)$ and $\mathbf{d}_{i,D,J_S}(k) - \mathbf{X}_{i,J_S}^T(k) \mathbf{w}(k+1)$ can be approximated by the a priori errors. Then we get

$$\Theta(k) = \|\mathbf{w}(k+1) - \mathbf{w}(k)\|^2 + \sum_{i=0}^{N-1} [\mathbf{e}_{i,D}^T(k) (\mathbf{X}_i^T(k) \mathbf{X}_i(k))^{-1} \mathbf{e}_{i,D}(k)], \quad (18)$$

and

$$\Theta_{J_S}(k) = \|\mathbf{w}(k+1) - \mathbf{w}(k)\|^2 + \sum_{i=0}^{N-1} [\mathbf{e}_{i,D,J_S}^T(k) (\mathbf{X}_{i,J_S}^T(k) \mathbf{X}_{i,J_S}(k))^{-1} \mathbf{e}_{i,D,J_S}(k)]. \quad (19)$$

Thus, the optimum selection of the input regressors is obtained by a subset that minimizes

$$J_S^{opt} = \left| \sum_{i=0}^{N-1} [\mathbf{e}_{i,D}^T(k) (\mathbf{X}_i^T(k) \mathbf{X}_i(k))^{-1} \mathbf{e}_{i,D}(k) - \mathbf{e}_{i,D,J_S}^T(k) (\mathbf{X}_{i,J_S}^T(k) \mathbf{X}_{i,J_S}(k))^{-1} \mathbf{e}_{i,D,J_S}(k)] \right|. \quad (20)$$

Since $\mathbf{e}_{i,D,J_S}^T(k) (\mathbf{X}_{i,J_S}^T(k) \mathbf{X}_{i,J_S}(k))^{-1} \mathbf{e}_{i,D,J_S}(k)$ is always smaller than $\mathbf{e}_{i,D}^T(k) (\mathbf{X}_i^T(k) \mathbf{X}_i(k))^{-1} \mathbf{e}_{i,D}(k)$, the optimum selection is reformulated by a subset that maximizes

$$J_S^{opt} = \sum_{i=0}^{N-1} [\mathbf{e}_{i,D,J_S}^T(k) (\mathbf{X}_{i,J_S}^T(k) \mathbf{X}_{i,J_S}(k))^{-1} \mathbf{e}_{i,D,J_S}(k)]. \quad (21)$$

To reduce the computational complexity of (21), we assume that the diagonal elements of $\mathbf{X}_{i,J_S}^T(k) \mathbf{X}_{i,J_S}(k)$ is much larger than off-diagonal elements [9]. Therefore, (21) is approximated for each subband as

$$\mathbf{e}_{i,D,J_S}^T(k) (\mathbf{X}_{i,J_S}^T(k) \mathbf{X}_{i,J_S}(k))^{-1} \mathbf{e}_{i,D,J_S}(k) \approx \frac{e_{i,D}^2(k-j_1)}{\|\mathbf{x}_i(k-j_1)\|^2} + \dots + \frac{e_{i,D}^2(k-j_S)}{\|\mathbf{x}_i(k-j_S)\|^2} \quad (22)$$

where $\mathbf{e}_{i,D}(k) = [e_{i,D}(k), e_{i,D}(k-1), \dots, e_{i,D}(k-P+1)]^T$. Based on (22), the indices of the optimum subset at each subband for every iteration are obtained by the following simplified procedure:

- 1) Compute the following values for $0 \leq j \leq P-1$ and $0 \leq i \leq N-1$

$$\frac{e_{i,D}^2(k-j)}{\|\mathbf{x}_i(k-j)\|^2}. \quad (23)$$

- 2) The j -indices of J_S^{opt} for each i correspond to the indices of the S largest values of (23).

Table I presents the pseudo-codes of SR-IMSAF.

IV. THE DSR-IMSAF ALGORITHM

In DSR-IMSAF, the number of selected input regressors at each subband are dynamically changed for every adaptation. By defining the weight error vector as $\tilde{\mathbf{w}}(k) = \mathbf{w}^o - \mathbf{w}(k)$, the weight error vector update equation in IMSAF can be stated as

$$\tilde{\mathbf{w}}(k+1) = \tilde{\mathbf{w}}(k) - \mu \sum_{i=0}^{N-1} \mathbf{X}_i(k) [\mathbf{X}_i^T(k) \mathbf{X}_i(k)]^{-1} \mathbf{e}_{i,D}(k). \quad (24)$$

Taking the squared Euclidean norm and then expectation from both sides of (24) lead to the mean-square deviation (MSD) that satisfies

$$E\{\|\tilde{\mathbf{w}}(k+1)\|^2\} = E\{\|\tilde{\mathbf{w}}(k)\|^2\} - \Delta, \quad (25)$$

where¹

$$\Delta = \sum_{i=0}^{N-1} [\mu(2-\mu) E\{\mathbf{e}_{i,D}^T(k) [\mathbf{X}_i^T(k) \mathbf{X}_i(k)]^{-1} \mathbf{e}_{i,D}(k)\} - 2\mu\sigma_{v_i,D}^2 \text{Tr}(E\{[\mathbf{X}_i^T(k) \mathbf{X}_i(k)]^{-1}\})]. \quad (26)$$

¹Please see Appendix A for more details.

TABLE I
THE SR-IMSAF ALGORITHM

<p>1. Initialization the parameters</p> <p>Initialization the parameters μ, ϵ, N, P, S</p> <p>Initialization $\mathbf{w}(-1) = \mathbf{0}$</p> <p>for $k = 0, 1, \dots$</p> <p style="padding-left: 2em;">for $i = 0, 1, \dots, N - 1$</p> <p style="padding-left: 4em;">$\mathbf{X}_i(k) = [\mathbf{x}_i(k), \mathbf{x}_i(k-1), \dots, \mathbf{x}_i(k-P+1)]^T$</p> <p style="padding-left: 4em;">$\mathbf{d}_{i,D}(k) = [d_{i,D}(k), d_{i,D}(k-1), \dots, d_{i,D}(k-P+1)]^T$</p> <p style="padding-left: 4em;">$\mathbf{e}_{i,D}(k) = \mathbf{d}_{i,D}(k) - \mathbf{X}_i^T(k)\mathbf{w}(k)$</p> <p>2. Determining the j-indices based on the S largest values</p> <p style="padding-left: 2em;">for $j = 0, 1, \dots, P - 1$</p> <p style="padding-left: 4em;">Compute the values $\frac{e_{i,D}^2(k-j)}{\ \mathbf{x}_i(k-j)\ ^2}$</p> <p style="padding-left: 4em;">end</p> <p>3. Update the input signal matrix and desired signal vector according to the selected regressors</p> <p style="padding-left: 2em;">$\mathbf{X}_{i,J_S}(k) = [\mathbf{x}_i(k-j_1), \mathbf{x}_i(k-j_2), \dots, \mathbf{x}_i(k-j_S)]$</p> <p style="padding-left: 2em;">$\mathbf{d}_{i,D,J_S}(k) = [d_{i,D}(k-j_1), \dots, d_{i,D}(k-j_S)]^T$</p> <p>4. Calculate the error vector</p> <p style="padding-left: 2em;">$\mathbf{e}_{i,D,J_S}(k) = \mathbf{d}_{i,D,J_S}(k) - \mathbf{X}_{i,J_S}^T(k)\mathbf{w}(k)$</p> <p>5. Update the filter coefficients</p> <p style="padding-left: 2em;">$\mathbf{w}(k+1) = \mathbf{w}(k) + \mu \sum_{i=0}^{N-1} \mathbf{X}_{i,J_S}(k)[\epsilon \mathbf{I} + \mathbf{X}_{i,J_S}^T(k)\mathbf{X}_{i,J_S}(k)]^{-1} \mathbf{e}_{i,D,J_S}(k)$</p> <p style="padding-left: 2em;">end</p> <p>end</p>
--

If Δ is maximized, then the fastest convergence is obtained. In (26), $\sigma_{v_{i,D}}^2$ is the variance of the i th subband signal of $v_i(k)$ being partitioned and decimated. Since the exact expected values are not available, the instantaneous values are used as follows

$$\hat{\Delta} = \mu(2 - \mu) \sum_{i=0}^{N-1} [\mathbf{e}_{i,D}^T(k) [\mathbf{X}_i^T(k) \mathbf{X}_i(k)]^{-1} \mathbf{e}_{i,D}(k) - \frac{2}{2 - \mu} \sigma_{v_{i,D}}^2 \text{Tr}([\mathbf{X}_i^T(k) \mathbf{X}_i(k)]^{-1})]. \quad (27)$$

Again we use the previous approximation for $\mathbf{X}_i^T(k) \mathbf{X}_i(k)$ and obtain [10]

$$\hat{\Delta} = \mu(2 - \mu) \sum_{i=0}^{N-1} \left\{ \left(\frac{e_{i,D}^2(k) - 2\sigma_{v_{i,D}}^2 / (2 - \mu)}{\|\mathbf{x}_i(k)\|^2} \right) + \left(\frac{e_{i,D}^2(k-1) - 2\sigma_{v_{i,D}}^2 / (2 - \mu)}{\|\mathbf{x}_i(k-1)\|^2} \right) + \dots \left(\frac{e_{i,D}^2(k-P+1) - 2\sigma_{v_{i,D}}^2 / (2 - \mu)}{\|\mathbf{x}_i(k-P+1)\|^2} \right) \right\}. \quad (28)$$

We can find the following facts. If at each subband $e_{i,D}^2(k-j) > 2\sigma_{v_{i,D}}^2/(2-\mu)$, then $\mathbf{x}_i(k-j)$ contributes to maximizing $\hat{\Delta}$. However, if $e_{i,D}^2(k-j) \leq 2\sigma_{v_{i,D}}^2/(2-\mu)$, then $\mathbf{x}_i(k-l)$ makes $\hat{\Delta}$ decrease. Therefore, we should perform the update with the input regressors satisfying $e_{i,D}^2(k-j) > 2\sigma_{v_{i,D}}^2/(2-\mu)$ at every iteration for the largest MSD decrease. Thus, the number of the selected input regressors at each subband for every iteration should be the same as the number of errors satisfying $e_{i,D}^2(k-j) > 2\sigma_{v_{i,D}}^2/(2-\mu)$.

Suppose $J_{S_i(k)} = \{j_1, j_2, \dots, j_{S_i(k)}\}$ indicates a subset with $S_i(k)$ members of the set $\{0, 1, \dots, P-1\}$ at each subband. Then, the update equation for proposed DSR-IMSAF is introduced as

$$\mathbf{w}(k+1) = \mathbf{w}(k) + \mu \sum_{i=0}^{N-1} \mathbf{X}_{i,J_{S_i(k)}}(k) [\epsilon \mathbf{I} + \mathbf{X}_{i,J_{S_i(k)}}^T(k) \mathbf{X}_{i,J_{S_i(k)}}(k)]^{-1} \mathbf{e}_{i,D,J_{S_i(k)}}(k), \quad (29)$$

where

$$\mathbf{e}_{i,D,J_{S_i(k)}}(k) = \mathbf{d}_{i,D,J_{S_i(k)}}(k) - \mathbf{X}_{i,J_{S_i(k)}}^T(k) \mathbf{w}(k), \quad (30)$$

and

$$\mathbf{e}_{i,D,J_{S_i(k)}}(k) = [e_{i,D}(k-j_1), \dots, e_{i,D}(k-j_{S_i(k)})]^T. \quad (31)$$

Also

$$\mathbf{X}_{i,J_{S_i(k)}}(k) = [\mathbf{x}_i(k-j_1) \dots \mathbf{x}_i(k-j_{S_i(k)})], \quad (32)$$

and

$$\mathbf{d}_{i,D,J_{S_i(k)}}(k) = [d_{i,D}(k-j_1), \dots, d_{i,D}(k-j_{S_i(k)})]. \quad (33)$$

The parameter $S_i(k)$ changes between 0 and P . The indices of the subset ($J_{S_i(k)}$) are obtained through the following procedure:

- 1) Compute the following values for $0 \leq j \leq P-1$ and $0 \leq i \leq N-1$

$$|e_{i,D}(k-j)| > \sqrt{\frac{2}{2-\mu}} \sigma_{v_{i,D}} \quad (34)$$

- 2) The j -indices of $J_{S_i(k)}$ at each subband correspond to the indices that satisfy the condition in (34).

Table II summarizes the pseudo-codes of DSR-IMSAF algorithm.

V. GENERAL UPDATE EQUATION

In [20], we showed that the update equation for the MSFAF can be expressed as

$$\mathbf{w}(k+1) = \mathbf{w}(k) + \mu \mathbf{X}(k) \mathbf{F}_1 [\epsilon \mathbf{I} + \text{diag}[\mathbf{F}_1^T \mathbf{X}^T(k) \mathbf{X}(k) \mathbf{F}_1]]^{-1} \mathbf{F}_1^T \mathbf{e}(k). \quad (35)$$

In (35), $\mathbf{F}_1 = [\mathbf{f}_0, \mathbf{f}_1, \dots, \mathbf{f}_{N-1}]$ is the $K \times N$ matrix, where \mathbf{f}_i is $K \times 1$ analysis filter bank at subband i , and

$$\mathbf{X}(k) = [\mathbf{x}(kN), \dots, \mathbf{x}(kN-K+1)]. \quad (36)$$

TABLE II
THE DSR-IMSAF ALGORITHM

<p>1. Initialization the parameters</p> <p>Initialization the parameters μ, ϵ, N, P</p> <p>Initialization $\mathbf{w}(-1) = \mathbf{0}$</p> <p>for $k = 0, 1, \dots$</p> <p style="padding-left: 2em;">for $i = 0, 1, \dots, N - 1$</p> <p style="padding-left: 4em;">$\mathbf{X}_i(k) = [\mathbf{x}_i(k), \mathbf{x}_i(k-1), \dots, \mathbf{x}_i(k-P+1)]^T$</p> <p style="padding-left: 4em;">$\mathbf{d}_{i,D}(k) = [d_{i,D}(k), d_{i,D}(k-1), \dots, d_{i,D}(k-P+1)]^T$</p> <p style="padding-left: 4em;">$\mathbf{e}_{i,D}(k) = \mathbf{d}_{i,D}(k) - \mathbf{X}_i^T(k)\mathbf{w}(k)$</p> <p>2. Determining the j-indices based on the the proposed condition</p> <p style="padding-left: 2em;">for $j = 0, 1, \dots, P - 1$</p> <p style="padding-left: 4em;">Compute the values $e_{i,D}(k-j) > \sqrt{\frac{2}{2-\mu}}\sigma_{v_{i,D}}$</p> <p style="padding-left: 4em;">end</p> <p>3. Update the input signal matrix and desired signal vector according to the selected regressors</p> <p style="padding-left: 2em;">$\mathbf{X}_{i,J_{S_i}(k)}(k) = [\mathbf{x}_i(k-j_1) \dots \mathbf{x}_i(k-j_{S_i}(k))]$</p> <p style="padding-left: 2em;">$\mathbf{d}_{i,D,J_{S_i}(k)}(k) = [d_{i,D}(k-j_1), \dots, d_{i,D}(k-j_{S_i}(k))]$</p> <p>4. Calculate the error vector</p> <p style="padding-left: 2em;">$\mathbf{e}_{i,D,J_{S_i}(k)}(k) = \mathbf{d}_{i,D,J_{S_i}(k)}(k) - \mathbf{X}_{i,J_{S_i}(k)}^T(k)\mathbf{w}(k)$</p> <p>5. Update the filter coefficients</p> <p style="padding-left: 2em;">$\mathbf{w}(k+1) = \mathbf{w}(k) + \mu \sum_{i=0}^{N-1} \mathbf{X}_{i,J_{S_i}(k)}(k)[\epsilon\mathbf{I} + \mathbf{X}_{i,J_{S_i}(k)}^T(k)\mathbf{X}_{i,J_{S_i}(k)}(k)]^{-1}\mathbf{e}_{i,D,J_{S_i}(k)}(k)$</p> <p style="padding-left: 2em;">end</p> <p>end</p>
--

Also, the error vector is given by

$$\mathbf{e}(k) = \mathbf{d}(k) - \mathbf{X}^T(k)\mathbf{w}(k), \quad (37)$$

where

$$\mathbf{d}(k) = [d(kN), d(kN-1), \dots, d(kN-K+1)]^T. \quad (38)$$

In the following, we will show that the IMSAF can also be incorporated in this framework. Focusing on (11) and following the straightforward analysis, the update equation for IMSAF can be established as

$$\mathbf{w}(k+1) = \mathbf{w}(k) + \mu \mathbf{X}(k) \mathbf{F}_P \{ \epsilon \mathbf{I} + \text{bdiag}[\mathbf{F}_P^T \mathbf{X}^T(k) \mathbf{X}(k) \mathbf{F}_P] \}^{-1} \mathbf{F}_P^T \mathbf{e}(k), \quad (39)$$

where now

$$\mathbf{X}(k) = [\mathbf{x}(kN), \mathbf{x}(kN - 1), \dots, \mathbf{x}((k - P + 1)N - K + 1)], \quad (40)$$

and

$$\mathbf{d}(k) = [d(kN), d(kN - 1), \dots, d((k - P + 1)N - K + 1)]^T. \quad (41)$$

The matrix \mathbf{F}_P is the $(K + (P - 1)N) \times PN$ matrix which is introduced as

$$\mathbf{F}_P = [\mathbf{f}_{0,P}, \mathbf{f}_{1,P}, \dots, \mathbf{f}_{N-1,P}], \quad (42)$$

where $\mathbf{f}_{i,P}$ is $(K + (P - 1)N) \times P$ matrix and is given by

$$\mathbf{f}_{i,P} = \begin{pmatrix} \mathbf{f}_i & \mathbf{0} & \dots & \mathbf{0} \\ \mathbf{0} & \mathbf{f}_i & \dots & \mathbf{0} \\ \vdots & \vdots & \ddots & \vdots \\ \mathbf{0} & \mathbf{0} & \dots & \dots \mathbf{f}_i \end{pmatrix}. \quad (43)$$

VI. EXTENSION OF THE FRAMEWORK

Based on (39), the SR-IMSAF and the DSR-IMSAF can be incorporated in the framework. Based on this extension, we can study the theoretical performance of introduced algorithms as well as IMSAF in a unified way.

A. SR-IMSAF

The SR-IMSAF algorithm in (17) can be remodeled as:

$$\mathbf{w}(k + 1) = \mathbf{w}(k) + \mu \mathbf{X}(k) \mathbf{F}_P \mathbf{B}(k) \{\epsilon \mathbf{I} + \text{bdiag}[\mathbf{B}^T(k) \mathbf{F}_P^T \mathbf{X}^T(k) \mathbf{X}(k) \mathbf{F}_P \mathbf{B}(k)]\}^{-1} \mathbf{B}^T(k) \mathbf{F}_P^T \mathbf{e}(k), \quad (44)$$

where $\mathbf{B}(k)$ is the $PN \times PN$ with the elements 1 and 0 on the diagonal. The positions of 1's on the diagonal determine which input regressors at each subband should be selected. The indices of these positions correspond to the condition in (23).

B. DSR-IMSAF

The new presentation for update equation in DSR-IMSAF is the same as (44). But the positions of 1's on the diagonal are determined based on the condition in (34).

VII. MEAN-SQUARE PERFORMANCE ANALYSIS OF THE FAMILY OF IMSAF ALGORITHMS

To study the performance of all proposed algorithms, we introduce a generic update equation as

$$\mathbf{w}(k + 1) = \mathbf{w}(k) + \mu \mathbf{C}(k) \mathbf{X}(k) \mathbf{W}(k) \mathbf{e}(k). \quad (45)$$

By selecting the proper matrices for $\mathbf{C}(k)$ and $\mathbf{W}(k)$ in (64), all proposed algorithms will be established. Table III shows the family of IMSAF algorithms. The transient behavior of an adaptive filter algorithm is determined by

TABLE III
THE FAMILY OF MSAF, IMSAF, SR-IMSAF, AND DSR-IMSAF ALGORITHMS

Algorithm	P	$\mathbf{C}(k)$	$\mathbf{W}(k)$
MSAF	$P = 1$	\mathbf{I}	$\mathbf{F}_1\{\epsilon\mathbf{I} + \text{diag}[\mathbf{F}_1^T\mathbf{X}^T(k)\mathbf{X}(k)\mathbf{F}_1]\}^{-1}\mathbf{F}_1^T$
IMSAF	$P \leq M$	\mathbf{I}	$\mathbf{F}_P\{\epsilon\mathbf{I} + \text{bdiag}[\mathbf{F}_P^T\mathbf{X}^T(k)\mathbf{X}(k)\mathbf{F}_P]\}^{-1}\mathbf{F}_P^T$
SR-IMSAF	$P \leq M$	\mathbf{I}	$\mathbf{F}_P\mathbf{B}(k)\{\epsilon\mathbf{I} + \text{bdiag}[\mathbf{B}^T(k)\mathbf{F}_P^T\mathbf{X}^T(k)\mathbf{X}(k)\mathbf{F}_P\mathbf{B}(k)]\}^{-1}\mathbf{B}^T(k)\mathbf{F}_P^T$
DSR-IMSAF	$P \leq M$	\mathbf{I}	$\mathbf{F}_P\mathbf{B}(k)\{\epsilon\mathbf{I} + \text{bdiag}[\mathbf{B}^T(k)\mathbf{F}_P^T\mathbf{X}^T(k)\mathbf{X}(k)\mathbf{F}_P\mathbf{B}(k)]\}^{-1}\mathbf{B}^T(k)\mathbf{F}_P^T$

the evolution of $E\{\|\tilde{\mathbf{w}}(k)\|_{\Phi}^2\}$, where $\tilde{\mathbf{w}}(k) = \mathbf{w}^o - \mathbf{w}(k)$ is the weight error vector and Φ is positive definite symmetric matrix. If $\Phi = \mathbf{R}$, where $\mathbf{R} = E\{\mathbf{x}(k)\mathbf{x}^T(k)\}$ is the autocorrelation matrix, the EMSE learning curve is obtained. For $\Phi = \mathbf{I}$, the MSD learning curve will be predicted. From (1) and (37), we obtain

$$\mathbf{e}(k) = \mathbf{X}^T(k)\tilde{\mathbf{w}}(k) + \mathbf{v}(k). \quad (46)$$

Therefore, the generic weight error vector update equation is given by

$$\tilde{\mathbf{w}}(k+1) = \tilde{\mathbf{w}}(k) - \mu\mathbf{C}(k)\mathbf{X}(k)\mathbf{W}(k)(\mathbf{X}^T(k)\tilde{\mathbf{w}}(k) + \mathbf{v}(k)). \quad (47)$$

By defining $\mathbf{Z}(k) = \mathbf{W}^T(k)\mathbf{X}^T(k)\mathbf{C}^T(k)$, the Φ -weighted norm of both sides of (47) is expressed as

$$\|\tilde{\mathbf{w}}(k+1)\|_{\Phi}^2 = \|\tilde{\mathbf{w}}(k)\|_{\Psi}^2 + \mu^2\mathbf{v}^T(k)\mathbf{Z}(k)\Phi\mathbf{Z}^T(k)\mathbf{v}(k) + \{\text{Crosstermsinvolving}\mathbf{v}(k)\}, \quad (48)$$

where

$$\Psi = \Phi - \mu\Phi\mathbf{Z}^T(k)\mathbf{X}^T(k) - \mu\mathbf{X}(k)\mathbf{Z}(k)\Phi + \mu^2\mathbf{X}(k)\mathbf{Z}(k)\Phi\mathbf{Z}^T(k)\mathbf{X}^T(k). \quad (49)$$

Taking the expectation from both sides of (48) yields

$$E\{\|\tilde{\mathbf{w}}(k+1)\|_{\Phi}^2\} = E\{\|\tilde{\mathbf{w}}(k)\|_{\Psi}^2\} + \mu^2E\{\mathbf{v}^T(k)\mathbf{Z}(k)\Phi\mathbf{Z}^T(k)\mathbf{v}(k)\}. \quad (50)$$

To simplify the recent relation, we apply the following independence assumptions [21]:

- 1) $\mathbf{X}(k)$ is independent and identically distributed sequence matrix. This assumption guarantees that $\tilde{\mathbf{w}}(k)$ is independent of both Ψ and $\mathbf{X}(k)$.
- 2) $\tilde{\mathbf{w}}(k)$ is independent of $\mathbf{Z}^T(k)\mathbf{X}^T(k)$.

Using these assumptions, the final result is

$$E\{\|\tilde{\mathbf{w}}(k+1)\|_{\Phi}^2\} = E\{\|\tilde{\mathbf{w}}(k)\|_{\Psi}^2\} + \mu^2E\{\mathbf{v}^T(k)\mathbf{Z}(k)\Phi\mathbf{Z}^T(k)\mathbf{v}(k)\}, \quad (51)$$

where

$$\Psi = \Phi - \mu\Phi E\{\mathbf{Z}^T(k)\mathbf{X}^T(k)\} - \mu E\{\mathbf{X}(k)\mathbf{Z}(k)\}\Phi + \mu^2 E\{\mathbf{X}(k)\mathbf{Z}(k)\Phi\mathbf{Z}^T(k)\mathbf{X}^T(k)\}. \quad (52)$$

Looking at the second term of the right-hand side of (52), we write

$$E\{\mathbf{v}^T(k)\mathbf{Z}(k)\Phi\mathbf{Z}^T(k)\mathbf{v}(k)\} = E\{\text{Tr}(\mathbf{v}(k)\mathbf{v}^T(k)\mathbf{Z}(k)\Phi\mathbf{Z}^T(k))\} = \text{Tr}(E\{\mathbf{v}(k)\mathbf{v}^T(k)\}E\{\mathbf{Z}(k)\Phi\mathbf{Z}^T(k)\}). \quad (53)$$

Since $E\{\mathbf{v}(k)\mathbf{v}^T(k)\} = \sigma_v^2\mathbf{I}$, equation (51) can be stated as

$$E\{\|\tilde{\mathbf{w}}(k+1)\|_{\Phi}^2\} = E\{\|\tilde{\mathbf{w}}(k)\|_{\Psi}^2\} + \mu^2\sigma_v^2\text{Tr}(E\{\mathbf{Z}(k)\Phi\mathbf{Z}^T(k)\}). \quad (54)$$

Applying the $\text{vec}(\cdot)$ operator on both sides of (52) and using $\text{vec}(\mathbf{P}\Sigma\mathbf{Q}) = (\mathbf{Q}^T \otimes \mathbf{P})\text{vec}(\Sigma)$ yield [22]

$$\psi = \phi - \mu(E\{\mathbf{X}(k)\mathbf{Z}(k)\} \otimes \mathbf{I})\cdot\phi - \mu(\mathbf{I} \otimes E\{\mathbf{X}(k)\mathbf{Z}(k)\})\cdot\phi + \mu^2(E\{(\mathbf{X}(k)\mathbf{Z}(k)) \otimes (\mathbf{X}(k)\mathbf{Z}(k))\})\cdot\phi, \quad (55)$$

where $\psi = \text{vec}(\Psi)$ and $\phi = \text{vec}(\Phi)$. By defining the $M^2 \times M^2$ matrix \mathbf{G} as

$$\mathbf{G} = \mathbf{I} - \mu E\{\mathbf{X}(k)\mathbf{Z}(k)\} \otimes \mathbf{I} - \mu \mathbf{I} \otimes E\{\mathbf{X}(k)\mathbf{Z}(k)\} + \mu^2 E\{(\mathbf{X}(k)\mathbf{Z}(k)) \otimes (\mathbf{X}(k)\mathbf{Z}(k))\}, \quad (56)$$

equation (55) becomes

$$\psi = \mathbf{G}\cdot\phi. \quad (57)$$

Also by defining γ through

$$\gamma = \text{vec}(E\{\mathbf{Z}^T(k)\mathbf{Z}(k)\}), \quad (58)$$

the second term of the right-hand side of (54) is given by

$$\text{Tr}(E\{\mathbf{Z}^T(k)\mathbf{Z}(k)\}\Phi) = \gamma^T\cdot\phi. \quad (59)$$

From the above analysis, the recursion of (54) is represented as

$$E\{\|\tilde{\mathbf{w}}(k+1)\|_{\Phi}^2\} = E\{\|\tilde{\mathbf{w}}(k)\|_{\mathbf{G}\phi}^2\} + \mu^2\sigma_v^2\gamma^T\phi. \quad (60)$$

Focusing again on the learning curve, we substitute \mathbf{R} for Φ , define $\mathbf{r} = \text{vec}(\mathbf{R})$, and write

$$E\{\|\tilde{\mathbf{w}}(k)\|_{\mathbf{r}}^2\} = E\{\|\tilde{\mathbf{w}}(0)\|_{\mathbf{G}^k\mathbf{r}}^2\} + \mu^2\sigma_v^2\gamma^T\{\mathbf{I} + \mathbf{G} + \dots + \mathbf{G}^{k-1}\}\mathbf{r}. \quad (61)$$

From this recursion, we will be able to obtain the steady-state excess mean square error (EMSE), when k goes to infinity. Doing this, the steady-state EMSE is established as

$$\text{EMSE} = \mu^2\sigma_v^2\gamma^T(\mathbf{I} - \mathbf{G})^{-1}\mathbf{r}. \quad (62)$$

When $\Phi = \mathbf{I}$, the transient behavior of mean square coefficient deviation (MSD) is predicted. The steady-state MSD is also given by

$$\text{MSD} = \mu^2\sigma_v^2\gamma^T(\mathbf{I} - \mathbf{G})^{-1}\text{vec}(\mathbf{I}). \quad (63)$$

VIII. MEAN AND MEAN-SQUARE STABILITY OF THE FAMILY OF IMSAF ALGORITHMS

Taking the expectation from both sides of (47) yields

$$E\{\tilde{\mathbf{w}}(k+1)\} = [\mathbf{I} - \mu E\{\mathbf{Z}^T(k)\mathbf{X}^T(k)\}]E\{\tilde{\mathbf{w}}(k)\}. \quad (64)$$

From (64), the convergence to the mean of the adaptive algorithm in (45) is guaranteed for any μ that satisfies

$$\mu < \frac{2}{\lambda_{\max}(E\{\mathbf{Z}^T(k)\mathbf{X}^T(k)\})}. \quad (65)$$

The general recursion (equation (60)) is stable if the matrix \mathbf{G} is stable [21]. From (56), we know that $\mathbf{G} = \mathbf{I} - \mu\mathbf{M} + \mu^2\mathbf{N}$, where $\mathbf{M} = E\{\mathbf{X}(k)\mathbf{Z}(k)\} \otimes \mathbf{I} + \mathbf{I} \otimes E\{\mathbf{X}(k)\mathbf{Z}(k)\}$, and $\mathbf{N} = E\{(\mathbf{X}(k)\mathbf{Z}(k)) \otimes (\mathbf{X}(k)\mathbf{Z}(k))\}$.

The condition on μ to guarantee the convergence in the mean-square sense of the adaptive algorithms is

$$0 < \mu < \min\left\{\frac{1}{\lambda_{\max}(\mathbf{M}^{-1}\mathbf{N})}, \frac{1}{\max(\lambda(\mathbf{H}) \in \mathfrak{R}^+)}\right\}, \quad (66)$$

where $\mathbf{H} = \begin{bmatrix} \frac{1}{2}\mathbf{M} & -\frac{1}{2}\mathbf{N} \\ \mathbf{I} & \mathbf{0} \end{bmatrix}$.

IX. COMPUTATIONAL COMPLEXITY

Table IV compares the computational complexity of the IMSAF, SR-IMSAF, and DSR-IMSAF algorithms in terms of the number of multiplications per iteration for real data. In this Table, M is the filter length, N is the number of subbands, P is the number of input regressors, L is the length of channel filters, S is the number of selected input regressors, and $S_i(k)$ is the number of selected regressors at each subband which is dynamic. This table indicates that the number of multiplications in IMSAF depends on P . But in SR-IMSAF and DSR-IMSAF, this parameter depends on S and $S_i(k)$. Also, the number of comparisons in SR-IMSAF and DSR-IMSAF is $O(P) + P\log_2 S$ and PN respectively [14]. In the next section, we also present the number of multiplications in different simulations.

TABLE IV
COMPUTATIONAL COMPLEXITY OF THE IMSAF, SR-IMSAF, AND DSR-IMSAF ALGORITHMS PER ITERATION

Algorithm	Number of Multiplications
IMSAF	$(P^2 + 2P)M + P^3 + P^2 + 3NL$
SR-IMSAF	$(S^2 + 2S)M + S^3 + S^2 + 2M(P - S) + 2P + 3NL$
DSR-IMSAF	$\sum_{i=0}^{N-1} \frac{1}{N} [(S_i^2(k) + S_i(k) + P)M + S_i^3(k) + S_i^2(k)] + 3NL$

TABLE V

TOTAL NUMBER OF MULTIPLICATIONS FOR IMSAF, SR-IMSAF, AND DSR-IMSAF ALGORITHMS UNTIL CONVERGENCE (INPUT SIGNAL: COLORED GAUSSIAN AR(2))

Algorithm	$N = 4, P = 4$	$N = 4, P = 8$	$N = 4, P = 16$
IMSAF	1.9×10^7	5.8×10^7	1.8×10^8
SR-IMSAF	1.3×10^7	3.6×10^7	9.4×10^7
DSR-IMSAF	5.8×10^6	1.3×10^7	1.9×10^7

TABLE VI

TOTAL NUMBER OF MULTIPLICATIONS FOR IMSAF, SR-IMSAF, AND DSR-IMSAF ALGORITHMS UNTIL CONVERGENCE (INPUT SIGNAL: REAL SPEECH)

Algorithm	$N = 4, P = 4$	$N = 4, P = 8$	$N = 4, P = 16$
IMSAF	9.4×10^8	1.4×10^9	2.8×10^9
SR-IMSAF	7.4×10^8	9×10^8	2.5×10^9
DSR-IMSAF	2.4×10^8	3.1×10^8	6.5×10^8

X. SIMULATION RESULTS

We demonstrate the performance of the proposed algorithms by several computer simulations in acoustic echo cancellation (AEC) setup. The impulse response of the car echo path with 256 taps ($M = 256$) is used as an unknown system in the experiment (Fig. 2) [23]. The input signal is an AR(2) signal which is generated by passing a zero-mean white Gaussian noise through a second-order system $\frac{1}{1-0.1z^{-1}-0.8z^{-2}}$ and the value of σ_v^2 is set to 10^{-3} . Also, the filter bank in all simulations is the extended lapped transform (ELT) [14], [24]. In all simulations, we show the normalized mean square deviation (NMSD), $E[\frac{\|\mathbf{w}^o - \mathbf{w}(k)\|^2}{\|\mathbf{w}^o\|^2}]$, which is evaluated by ensemble averaging over 50 independent trials.

A. Performance of the Algorithms

Fig. 3 shows the NMSD learning curves of IMSAF and SR-IMSAF algorithms. The parameters μ , ϵ , and N are set 0.5, 0.01, and 4, respectively. To make the computational complexity similar, the parameter P in conventional IMSAF is set to 4 and this parameter in SR-IMSAF is set to 8 and 16 where $S = 4$. Therefore, only 4 regressors are selected at each subband in SR-IMSAF during the adaptation. We observe that the SR-IMSAF has faster convergence speed than IMSAF while the computational complexity is similar.

Fig. 4 presents the NMSD learning curves of IMSAF and DSR-IMSAF algorithms. The step-size is set to 0.5 and various values for P are selected in IMSAF algorithm (2, 4, 8, 16, and 32). In conventional IMSAF, by increasing the parameter P , the convergence speed and steady-state error are increased. For DSR-IMSAF, we set the parameter

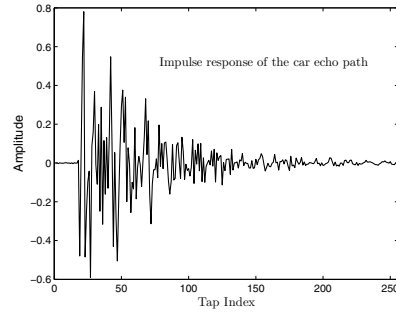


Fig. 2. Impulse response of the car echo path ($M = 256$).

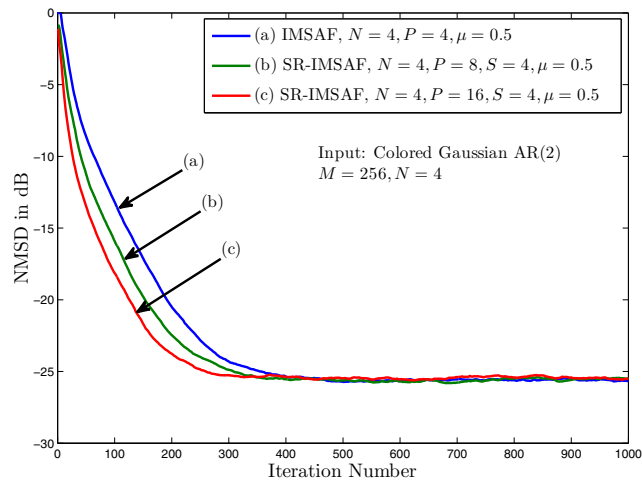


Fig. 3. The NMSD learning curves of IMSAF and SR-IMSAF (Input signal: Colored Gaussian AR(2)).

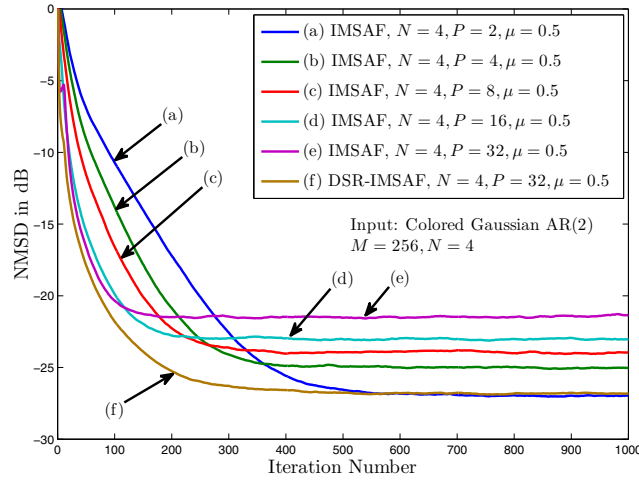


Fig. 4. The NMSD learning curves of IMSAF and DSR-IMSAF (Input signal: Colored Gaussian AR(2)).

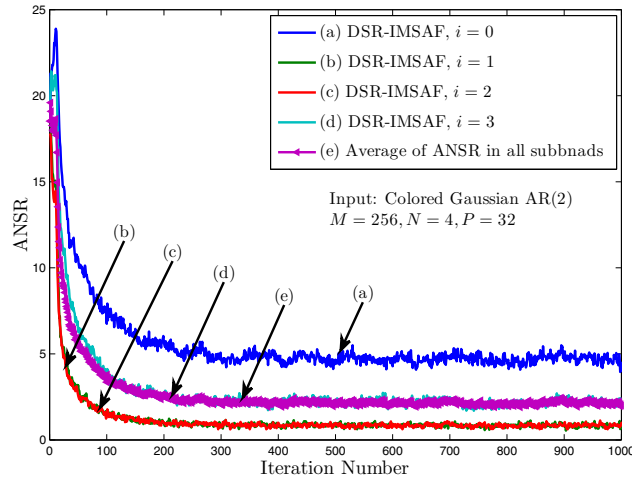


Fig. 5. The average number of selected regressors (ANSR) for DSR-IMSAF in different subbands with $P = 32$.

P to 32. In this case, the convergence speed of the proposed DSR-IMSAF is the same as the conventional IMSAF with the maximum order, which has the fast convergence speed, while the steady-state error remains low. Fig. 5 shows the average number of selected regressors (ANSR) in DSR-IMSAF for different subbands. This figure indicates that the number of selected regressors is dynamically decreased in all subbands. Therefore, the proposed DSR-IMSAF has a low overall computational complexity because the average number of selected regressors in all subbands is small. In Fig. 6, the performances of DSR-IMSAF based on Eqs. 27 and 28 are presented. In this simulation, we set P to 4. Eq. 27 uses the all elements of $\mathbf{X}_i^T(k)\mathbf{X}_i(k)$ and Eq. 28 applies only the diagonal elements of $\mathbf{X}_i^T(k)\mathbf{X}_i(k)$. The NMSD learning curves show that the performances of DSR-IMSAF based on these relations are close together.

Figs. 7 and 8 show the performance of SR-IMSAF for different values of P . In Fig. 7, the step-size is set 0.5

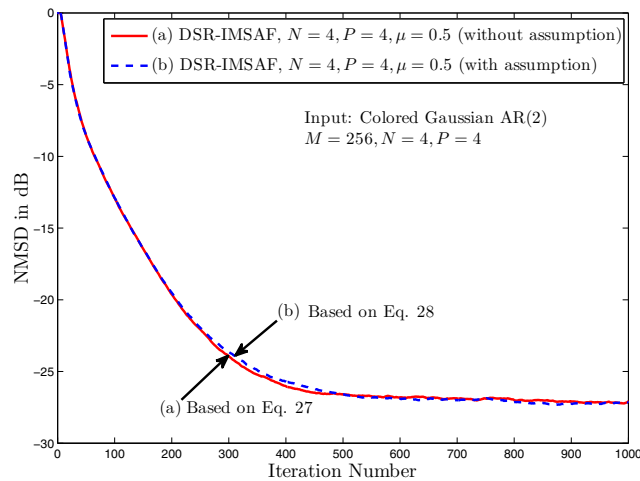


Fig. 6. The NMSD learning curves of DSR-IMSAF with $P = 4$ based on Eqs. 27 and 28.

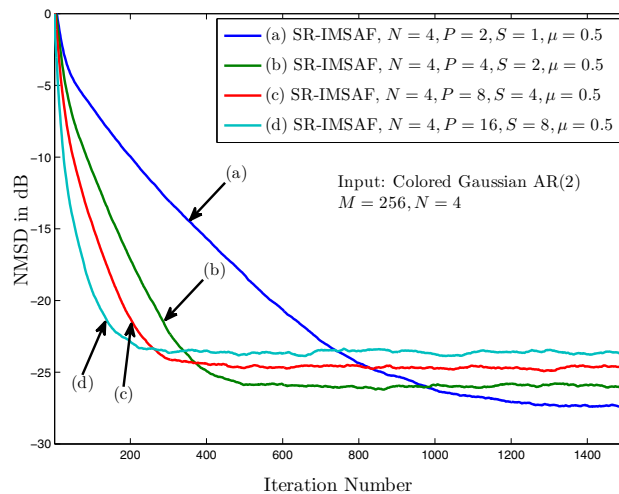


Fig. 7. The NMSD learning curves of SR-IMSAF for different values of P and $\mu = 0.5$ (Input signal: Colored Gaussian AR(2)).

and P is selected as 2, 4, 8, and 16. The value of S is chosen as $P/2$. By increasing P , the convergence speed and the steady-state error increase. In Fig. 8, the step-size is set to 0.5 in SR-IMSAF with $P = 2$ and to make the comparison fair, the step-sizes for SR-IMSAF with other values of P are chosen to get approximately the same steady-state NMSD as SR-IMSAF with $P = 2$. As we see, by increasing P , the convergence speed increases. Figs. 9 and 10 present the results for DSR-IMSAF. The NMSD learning curves indicate that by increasing the parameter P , the convergence speed are increased.

Fig. 11 compares the performance of APA, MSAF, IMSAF, SR-IMSAF, and DSR-IMSAF algorithms. The values of N and P are set to 4. The step-size is set to 0.5 in MSAF and to make the comparison fair, the step-sizes for other algorithms are chosen to get approximately the same steady-state NMSD as MSAF. As we see, the convergence performance of the proposed SR-IMSAF and DSR-IMSAF is comparable to the conventional IMSAF

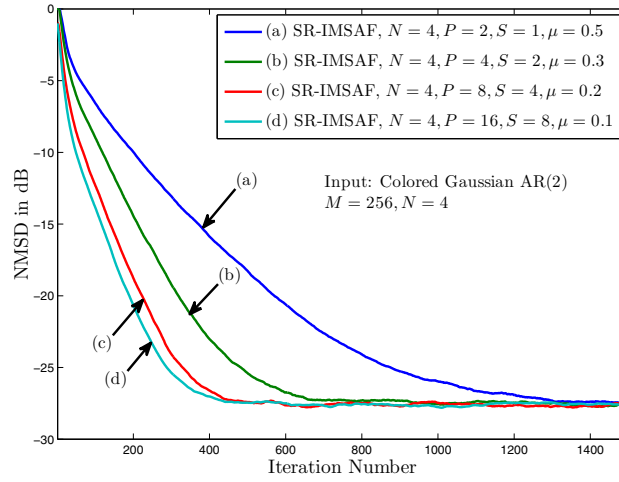


Fig. 8. The NMSD learning curves of SR-IMSAF for different values of P with the same steady-state error (Input signal: Colored Gaussian AR(2)).

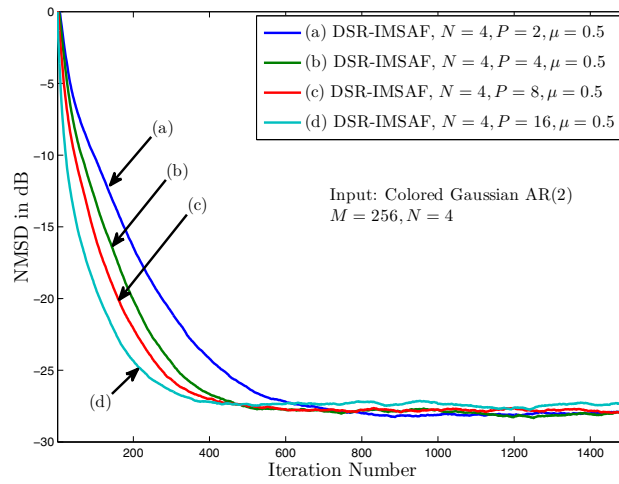


Fig. 9. The NMSD learning curves of DSR-IMSAF for different values of P and $\mu = 0.5$ (Input signal: Colored Gaussian AR(2)).

while the proposed SR-IMSAF and DSR-IMSAF have a better computational superiority. Fig. 12 shows the ANSR for different subbands in DSR-IMSAF. The proposed DSR-IMSAF has a low overall computational complexity because the average number of the selected input vectors is small in all subbands. Figs. 13 and 14 present the same results for $P = 8$. Again good performance is observed for the proposed algorithms. The good performance of the proposed algorithms for $P = 16$ is given in Figs. 15 and 16. Table V compares the number of multiplications until convergence in IMSAF, SR-IMSAF, and DSR-IMSAF. This table shows that the computational complexity of SR-IMSAF and DSR-IMSAF is lower than IMSAF. As we see, the number of multiplications in DSR-IMSAF with $P = 16$ is even lower than IMSAF with $P = 4$. In Figs. 17 and 18, the input signal is changed to colored Gaussian AR(1) with transfer function $\frac{1}{1-\rho z^{-1}}$, where ρ is set to 0.9 and 0.95. The parameters in this figure are

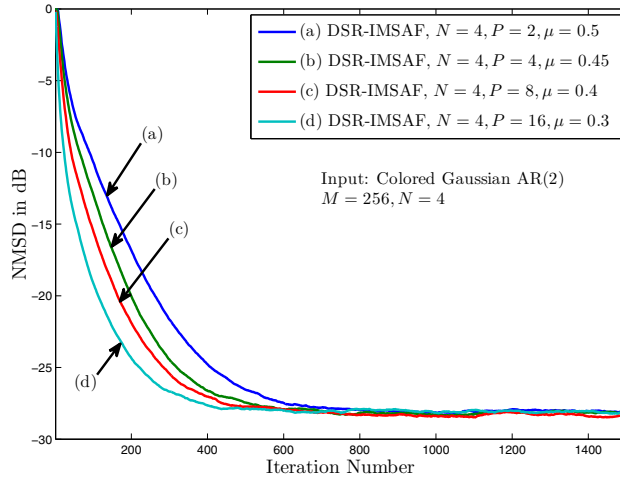


Fig. 10. The NMSD learning curves of DSR-IMSAF for different values of P with the same steady-state error (Input signal: Colored Gaussian AR(2)).

chosen according to Fig. 11. We observe good performance for the proposed algorithms in both input signals. In Fig. 19, the performance of IMSAF algorithm based on Eqs. (11) and (39) is compared. The parameter N is set to 4 and different values for P are selected. As we see, the same performance is achieved through these relations.

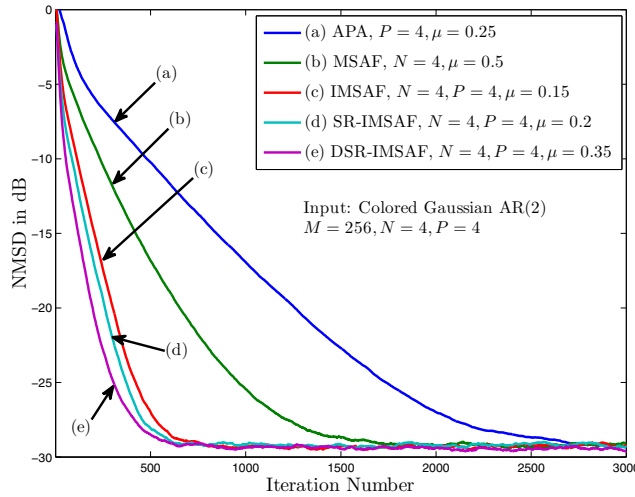


Fig. 11. The NMSD learning curves of APA, MSAF, IMSAF, SR-IMSAF, and DSR-IMSAF with $P = 4$ (Input signal: Colored Gaussian AR(2)).

For tracking performance analysis, we consider a system to identify the two unknown filters with $M = 256$, whose z-domain transfer functions are given by

$$\mathbf{W}_1(z) = \sum_{n=0}^{127} z^{-n} - \sum_{n=128}^{M-1} z^{-n}, \quad (67)$$

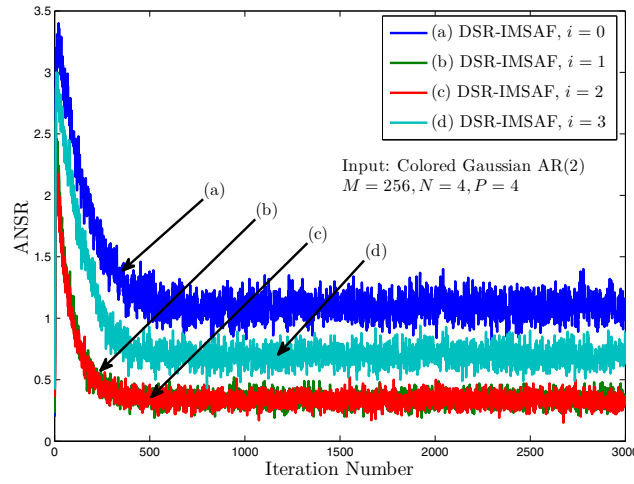


Fig. 12. The average number of selected regressors (ANSR) for DSR-IMSAF in different subbands with $P = 4$.

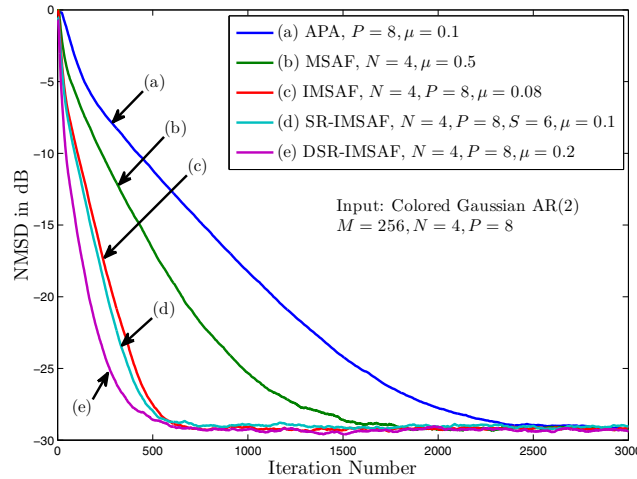


Fig. 13. The NMSD learning curves of APA, MSAF, IMSAF, SR-IMSAF, and DSR-IMSAF with $P = 8$ (Input signal: Colored Gaussian AR(2)).

and

$$\mathbf{W}_2(z) = - \sum_{n=0}^{M-1} z^{-n}, \quad (68)$$

where the transfer function of optimum filter coefficients will be $\mathbf{W}_1(z)$ for $n \leq 5 \times 10^3$, and the transfer function of optimum filter coefficients will be $\mathbf{W}_2(z)$ for $5 \times 10^3 < n \leq 10 \times 10^3$. Fig. 20 compares the tracking performance of APA, MSAF, IMSAF, SR-IMSAF, and DSR-IMSAF algorithms. The values of N and P are set to 4. The step-size in MSAF is set to 0.5 and to make the comparison fair, the step-sizes for other algorithms are chosen to get approximately the same steady-state NMSD as MSAF. The tracking performance of the introduced algorithms is the same as the conventional IMSAF while the proposed algorithms have a low overall computational complexity. In

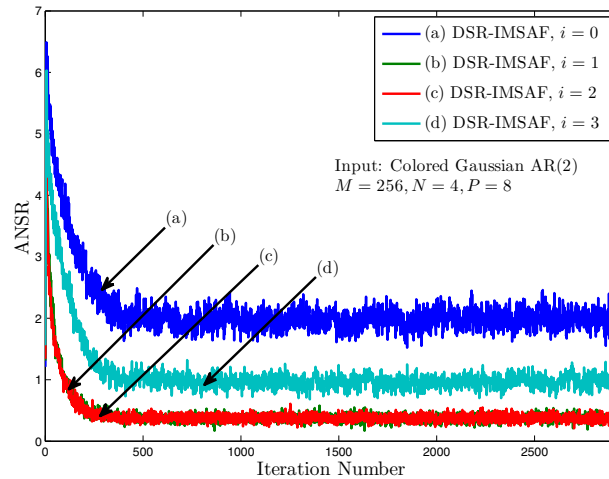


Fig. 14. The average number of selected regressors (ANSR) for DSR-IMSAF in different subbands with $P = 8$.

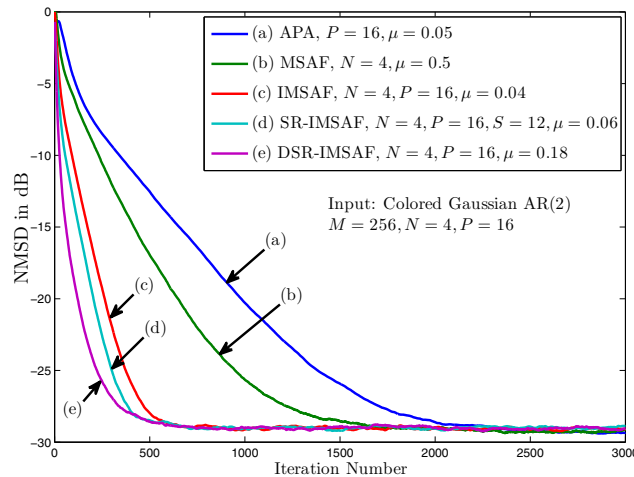


Fig. 15. The NMSD learning curves of APA, MSAF, IMSAF, SR-IMSAF, and DSR-IMSAF with $P = 16$ (Input signal: Colored Gaussian AR(2)).

Fig. 21, the tracking performance of IMSAF, SR-IMSAF, and DSR-IMSAF is compared. In IMSAF, the parameter P is set 16. To have a similar complexity with IMSAF, P and S are set 32 and 16 in SR-IMSAF. Also, the NMSD learning curves of DSR-IMSAF with $P = 16$ and 32 are presented. The learning curves show that the tracking performance of the proposed algorithms are better than conventional IMSAF.

In the following, we present the NMSD learning curves of the proposed algorithms for real speech input signal. The parameters μ , ϵ , and N are set to 0.05, 0.5, and 4. Fig. 22 compares the performance of APA, MSAF, IMSAF, SR-IMSAF, and DSR-IMSAF with $P = 4$. We observe that the performance of the proposed algorithms is close to the conventional IMSAF. Figs. 23 and 24 present the learning curves for $P = 8$ and 16. The same performance is observed in these figures. Table VI shows the number of multiplications in IMSAF, SR-IMSAF, and DSR-

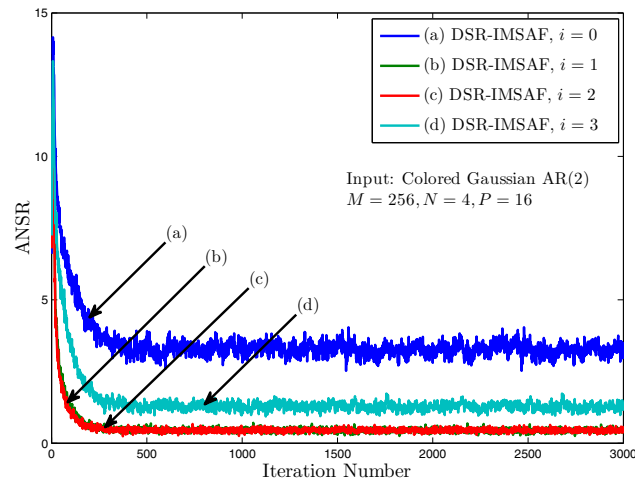


Fig. 16. The average number of selected regressors (ANSR) for DSR-IMSAF in different subbands with $P = 16$.

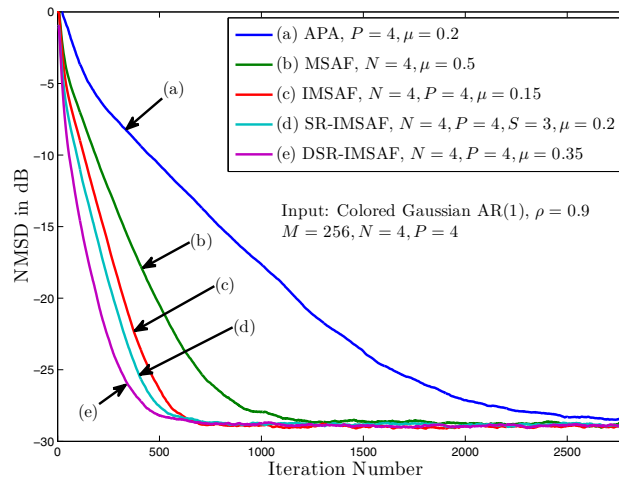


Fig. 17. The NMSD learning curves of APA, MSFAF, IMSAF, SR-IMSAF, and DSR-IMSAF with $P = 4$ (Input signal: Colored Gaussian AR(1), $\rho = 0.9$).

IMSAF, when the NMSD arrives to -18dB . As we see, the computational load of DSR-IMSAF is significantly lower than IMSAF. Also, to measure the effectiveness of the proposed algorithms, we compute the echo return loss enhancement (ERLE). The ERLE is obtained by evaluating the difference between the powers of the echo and the error signal. The segmental ERLE estimates are obtained by averaging over 140 samples. The segmental ERLE curves for the measured speech and echo signals are shown in Figs. 25 and 26. These figures illustrate that the proposed algorithms and conventional IMSAF have comparable ERLE performance.

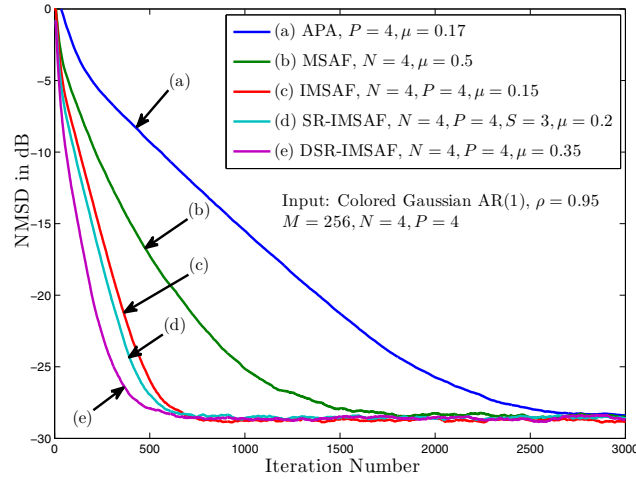


Fig. 18. The NMSD learning curves of APA, MSAF, IMSAF, SR-IMSAF, and DSR-IMSAF with $P = 4$ (Input signal: Colored Gaussian AR(1), $\rho = 0.95$).

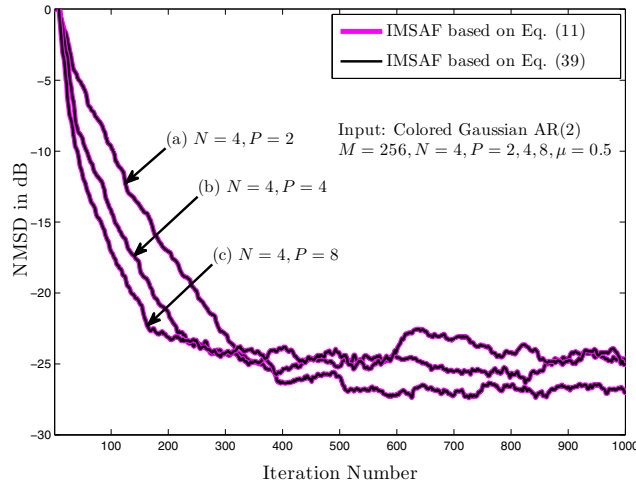


Fig. 19. The NMSD learning curves of IMSAF with $N = 4$, $P = 2, 4, 8$ based on Eqs. (11) and (39) (Input signal: Colored Gaussian AR(2)).

B. Transient Performance

To justify the theoretical results, we present the simulated and theoretical NMSD learning curves. The unknown impulse response is randomly selected with 32 taps ($M = 32$). The input signal is an AR(1) signal generated by passing a zero-mean white Gaussian noise through a first-order system $H(z) = \frac{1}{1-0.95z^{-1}}$ and the value of σ_v^2 is set to 10^{-3} . The theoretical learning curves are obtained from (61). The simulated learning curves are established by ensemble averaging over 30 independent trials. Fig. 27 presents the simulated and theoretical learning curves for SR-IMSAF with $S = 3$ and different values of P . Good agreement between simulated and theoretical learning curve is observed. The results for DSR-IMSAF can be seen in Fig. 28 for various values of P . As we can see,

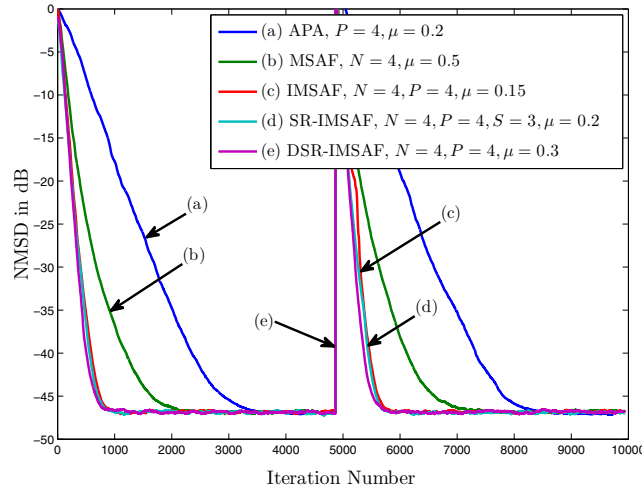


Fig. 20. Tracking performance of APA, MSAF, IMSAF, SR-IMSAF, and DSR-IMSAF with $P = 4$ (Input signal: Colored Gaussian AR(2)).

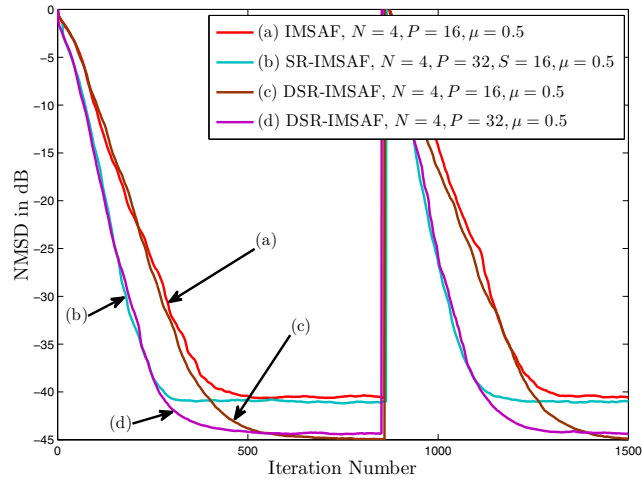


Fig. 21. Tracking performance of IMSAF, SR-IMSAF, and DSR-IMSAF (Input signal: Colored Gaussian AR(2)).

there is good agreement between simulated and theoretical learning curves.

C. Steady-State Performance

Figs. 29-31 show the simulated and theoretical steady-state NMSD values as function of the step-size for the proposed algorithms. The theoretical values are calculated from (63) and the simulated values are obtained from the averaging over 500 steady-state samples from 500 independent realizations for each value of μ for a given algorithm. The values of the step-size change in the stability bounds. Fig. 29 shows the results for IMSAF algorithms for two different values of P . As we can see, there is good agreement between simulated and theoretical values for both values of P . Fig. 30 presents the steady-state NMSD values as a function of the step-size for SR-IMSAF. In this algorithm, for $P = 4$, the parameter S is set to 3 and for $P = 8$, the parameter S is set 6. In both figures, the

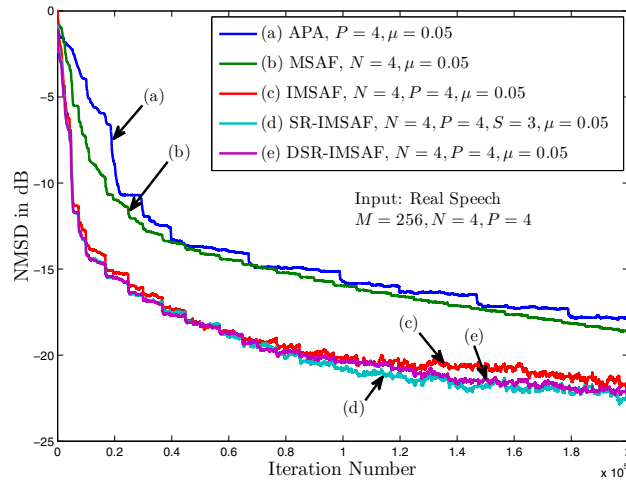


Fig. 22. The NMSD learning curves of IMSAF, SR-IMSAF, and DSR-IMSAF with $P = 4$ (Input signal: Real speech).

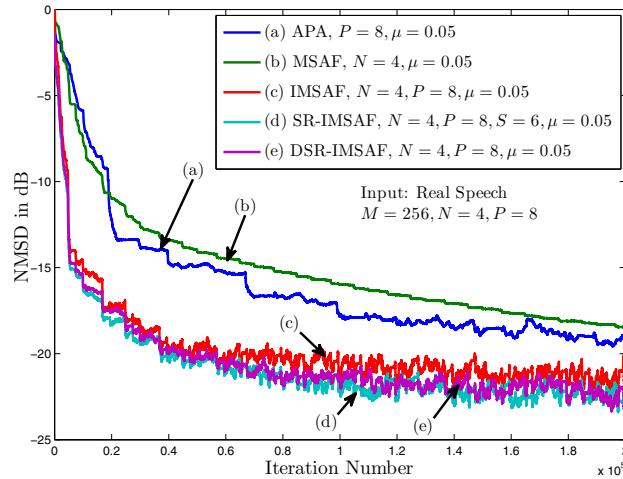


Fig. 23. The NMSD learning curves of APA, MSAF, IMSAF, SR-IMSAF, and DSR-IMSAF with $P = 8$ (Input signal: Real speech).

agreements are good. Finally, in Fig. 31, the results for DSR-IMSAF with $P = 4$ and 8 are shown. The agreement is well in this figure for both values of P .

D. Stability Bounds

Figs. 32-34 present the simulated steady-state NMSD values as a function of the step-size for the proposed algorithms with various values of P . The step-size changes from 0.05 to μ_{max} . The values of the μ_{max} are obtained from (65) and (66) which are presented in Table VII. Fig. 32 presents the results for IMSAF, SR-IMSAF and DSR-IMSAF algorithms with $P = 4$. Figs. 33 and 34 show the same curves for $P = 8$ and 16. We can see good agreement between the stability bounds from Table VII and the simulated steady-state NMSD for μ_{max} in all figures.

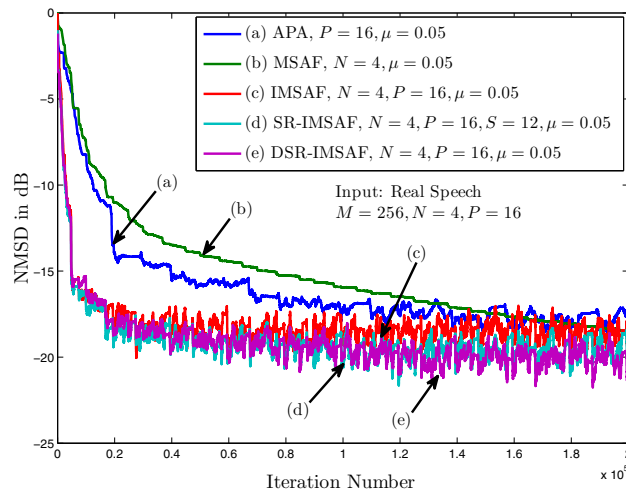


Fig. 24. The NMSD learning curves of APA, MSAF, IMSAF, SR-IMSAF, and DSR-IMSAF with $P = 16$ (Input signal: Real speech).

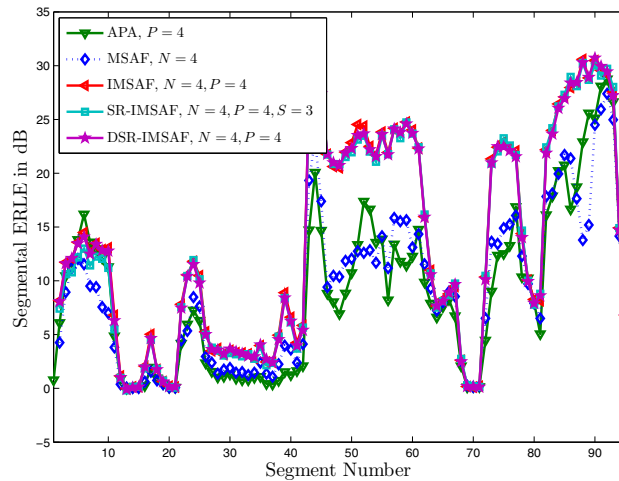


Fig. 25. Segmental ERLE curves of APA, MSAF, IMSAF, SR-IMSAF, and DSR-IMSAF with $P = 4$.

XI. CONCLUSION

This paper proposed two new adaptive filter algorithms with low computational complexity feature. These algorithms utilized the SR and DSR approaches in IMSAF algorithm. In SR-IMSAF, a subset of input regressors was optimally selected at each subband for every iteration. The dynamic selection of input regressors at each subband was performed in DSR-IMSAF algorithm. The introduced algorithms have shown good convergence performance with significantly reduced complexity. In the following, the general update equation for establishment of the proposed algorithms was introduced. Based on this, a unified approach for performance analysis of all algorithms was presented. The theoretical relations for transient, steady-state, and stability bounds were derived. Good performances of SR-IMSAF and DSR-IMSAF algorithms and the validity of the theoretical relations were

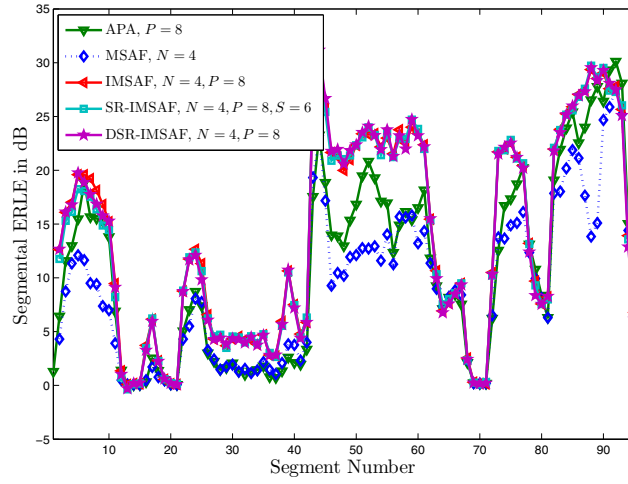


Fig. 26. Segmental ERLE curves of APA, MSAF, IMSAF, SR-IMSAF, and DSR-IMSAF with $P = 8$.

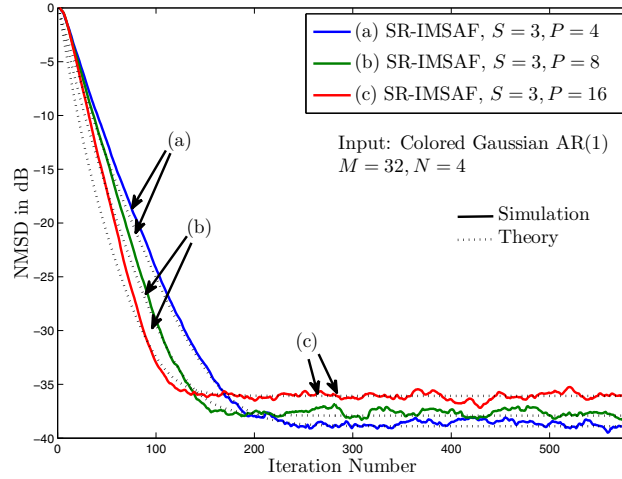


Fig. 27. The simulated and theoretical NMSD learning curves of SR-IMSAF for $P = 4, 8,$ and 16 (Input signal: Colored Gaussian AR(1)).

justified through several experiments.

APPENDIX A

DERIVATION OF EQ. 26

Taking the squared Euclidean norm and then expectation from both sides of (24) yield

$$\begin{aligned}
 E\{\|\tilde{\mathbf{w}}(k+1)\|^2\} &= E\{\|\tilde{\mathbf{w}}(k)\|^2\} - 2\mu \sum_{i=0}^{N-1} E\{\tilde{\mathbf{w}}^T(k) \mathbf{X}_i(k) [\mathbf{X}_i^T(k) \mathbf{X}_i(k)]^{-1} \mathbf{e}_{i,D}(k)\} \\
 &\quad + \mu^2 \sum_{i=0}^{N-1} E\{\mathbf{e}_{i,D}^T(k) [\mathbf{X}_i^T(k) \mathbf{X}_i(k)]^{-1} \mathbf{e}_{i,D}(k)\}. \tag{69}
 \end{aligned}$$

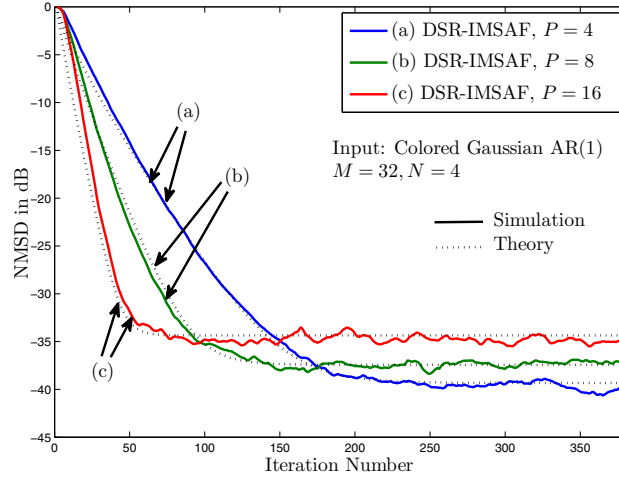


Fig. 28. The simulated and theoretical NMSD learning curves of DSR-IMSAF for $P = 4, 8,$ and 16 (Input signal: Colored Gaussian AR(1)).

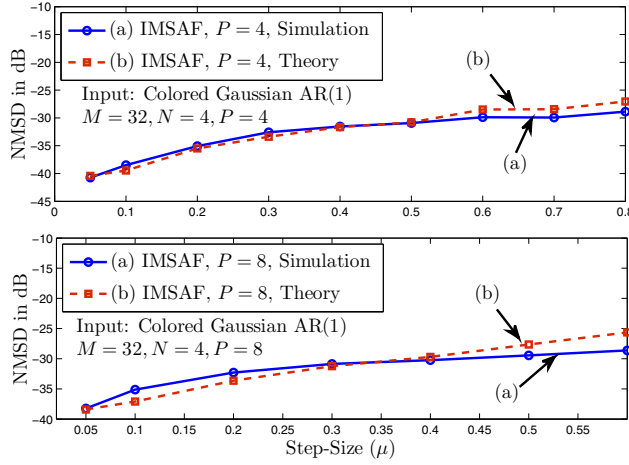


Fig. 29. The simulated and theoretical steady-state NMSD values of IMSAF as a function of the step-size for $P = 4$ and 8 (Input signal: Colored Gaussian AR(1)).

Since $\mathbf{X}_i^T(k)\tilde{\mathbf{w}}(k) = \mathbf{e}_{i,D}(k) - \mathbf{v}_{i,D}(k)$, we have

$$\begin{aligned}
 E\{\|\tilde{\mathbf{w}}(k+1)\|^2\} &= E\{\|\tilde{\mathbf{w}}(k)\|^2\} - 2\mu \sum_{i=0}^{N-1} E\{(\mathbf{e}_{i,D}^T(k) - \mathbf{v}_{i,D}^T(k))[\mathbf{X}_i^T(k)\mathbf{X}_i(k)]^{-1}\mathbf{e}_{i,D}(k)\} \\
 &\quad + \mu^2 \sum_{i=0}^{N-1} E\{\mathbf{e}_{i,D}^T(k)[\mathbf{X}_i^T(k)\mathbf{X}_i(k)]^{-1}\mathbf{e}_{i,D}(k)\} \quad (70)
 \end{aligned}$$

Therefore,

$$E\{\|\tilde{\mathbf{w}}(k+1)\|^2\} = E\{\|\tilde{\mathbf{w}}(k)\|^2\} - 2\mu \sum_{i=0}^{N-1} E\{\mathbf{e}_{i,D}^T(k)[\mathbf{X}_i^T(k)\mathbf{X}_i(k)]^{-1}\mathbf{e}_{i,D}(k)\}$$

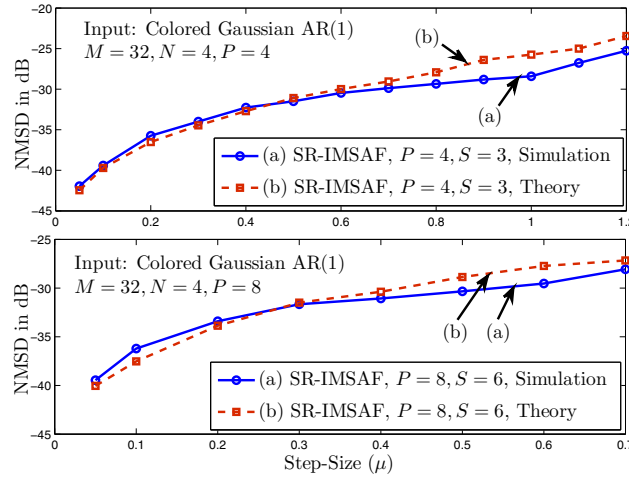


Fig. 30. The simulated and theoretical steady-state NMSD values of SR-IMSAF as a function of the step-size for $P = 4$ and 8 (Input signal: Colored Gaussian AR(1)).

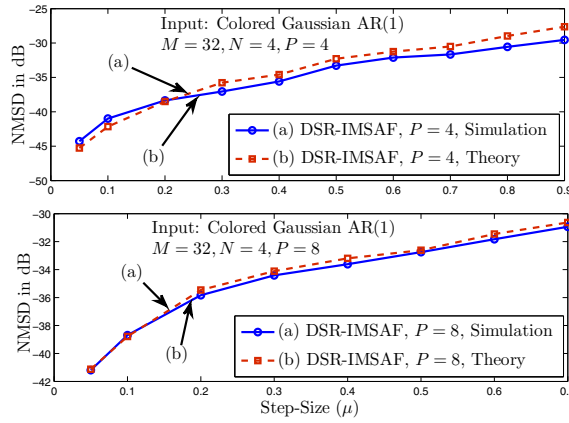


Fig. 31. The simulated and theoretical steady-state NMSD values of DSR-IMSAF as a function of the step-size for $P = 4$ and 8 (Input signal: Colored Gaussian AR(1)).

$$+2\mu \sum_{i=0}^{N-1} E\{\mathbf{v}_{i,D}^T(k)[\mathbf{X}_i^T(k)\mathbf{X}_i(k)]^{-1}\mathbf{e}_{i,D}(k)\} + \mu^2 \sum_{i=0}^{N-1} E\{\mathbf{e}_{i,D}^T(k)[\mathbf{X}_i^T(k)\mathbf{X}_i(k)]^{-1}\mathbf{e}_{i,D}(k)\}. \quad (71)$$

The third term in the right-hand side of Eq. 71 can be written as

$$\sum_{i=0}^{N-1} E\{\mathbf{v}_{i,D}^T(k)[\mathbf{X}_i^T(k)\mathbf{X}_i(k)]^{-1}\mathbf{e}_{i,D}(k)\} = \sum_{i=0}^{N-1} E\{\mathbf{v}_{i,D}^T(k)[\mathbf{X}_i^T(k)\mathbf{X}_i(k)]^{-1}[\mathbf{X}_i^T(k)\tilde{\mathbf{w}}(k) + \mathbf{v}_{i,D}(k)]\} \quad (72)$$

Assuming $v_{i,D}(k)$ is as zero mean and independent and identically distributed (i.i.d) sequence which is statistically independent of the input data, and by neglecting the dependency of $\tilde{\mathbf{w}}(k)$ on the past noise, Eq. 72 is obtained as

$$\sum_{i=0}^{N-1} E\{\mathbf{v}_{i,D}^T(k)[\mathbf{X}_i^T(k)\mathbf{X}_i(k)]^{-1}\mathbf{e}_{i,D}(k)\} = \sum_{i=0}^{N-1} E\{\mathbf{v}_{i,D}^T(k)[\mathbf{X}_i^T(k)\mathbf{X}_i(k)]^{-1}\mathbf{v}_{i,D}(k)\}. \quad (73)$$

TABLE VII

STABILITY BOUNDS OF THE IMSAF, SR-IMSAF AND DSR-IMSAF ALGORITHMS FOR $N = 4$ AND DIFFERENT VALUES OF P (INPUT SIGNAL: COLORED GAUSSIAN AR(2))

Algorithm	$\frac{2}{\lambda_{\max}(E\{\text{sgn}(\mathbf{X}(k)\mathbf{F})\mathbf{W}(k)\mathbf{F}^T\mathbf{X}^T(k)\})}$	$\frac{1}{\lambda_{\max}(\mathbf{M}^{-1}\mathbf{N})}$	$\frac{1}{\max(\lambda(\mathbf{H}) \in \mathfrak{R}^+)}$	μ_{max}
IMSAF ($N = 4, P = 4$)	2.1287	0.8098	2.126	0.8098
IMSAF ($N = 4, P = 8$)	1.7120	0.6169	1.1814	0.6169
IMSAF ($N = 4, P = 16$)	0.7180	0.5336	0.6828	0.5336
SR-IMSAF ($N = 4, P = 4$)	2.8135	1.3575	3.902	1.3575
SR-IMSAF ($N = 4, P = 8$)	1.8294	1.2263	2.6794	1.2263
SR-IMSAF ($N = 4, P = 16$)	0.8826	0.8372	1.4723	0.8372
DSR-IMSAF ($N = 4, P = 4$)	2.2316	0.9173	2.177	0.9173
DSR-IMSAF ($N = 4, P = 8$)	1.5674	0.7667	1.2386	0.7667
DSR-IMSAF ($N = 4, P = 16$)	0.7991	0.6270	0.7616	0.6270

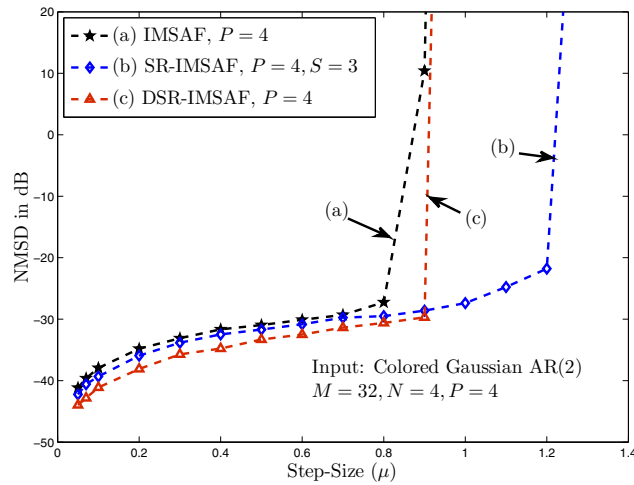


Fig. 32. The simulated steady-state NMSD values of IMSAF, SR-IMSAF, and DSR-IMSAF as a function of the step-size for $P = 4$ (Input signal: Colored Gaussian AR(2)).

Eq. 73 can be simplified as

$$\begin{aligned}
 \sum_{i=0}^{N-1} E\{\mathbf{v}_{i,D}^T(k)[\mathbf{X}_i^T(k)\mathbf{X}_i(k)]^{-1}\mathbf{v}_{i,D}(k)\} &= \sum_{i=0}^{N-1} E\{\text{Tr}(\mathbf{v}_{i,D}(k)\mathbf{v}_{i,D}^T(k)[\mathbf{X}_i^T(k)\mathbf{X}_i(k)]^{-1})\} \\
 &= \sum_{i=0}^{N-1} \text{Tr}(E\{\mathbf{v}_{i,D}(k)\mathbf{v}_{i,D}^T(k)\}E\{[\mathbf{X}_i^T(k)\mathbf{X}_i(k)]^{-1}\}). \quad (74)
 \end{aligned}$$

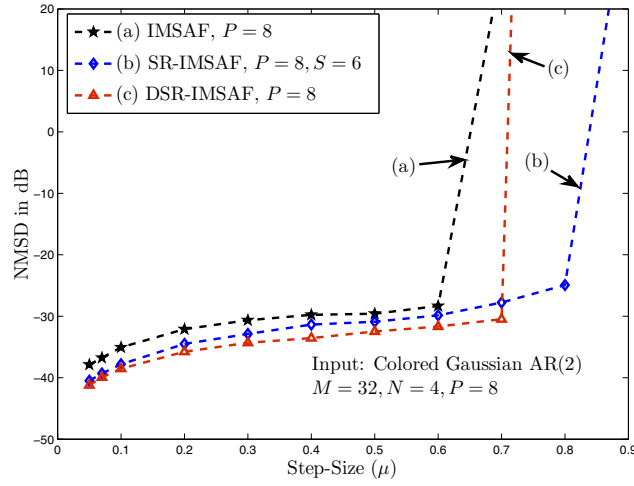


Fig. 33. The simulated steady-state NMSD values of IMSAF, SR-IMSAF, and DSR-IMSAF as a function of the step-size for $P = 8$ (Input signal: Colored Gaussian AR(2)).

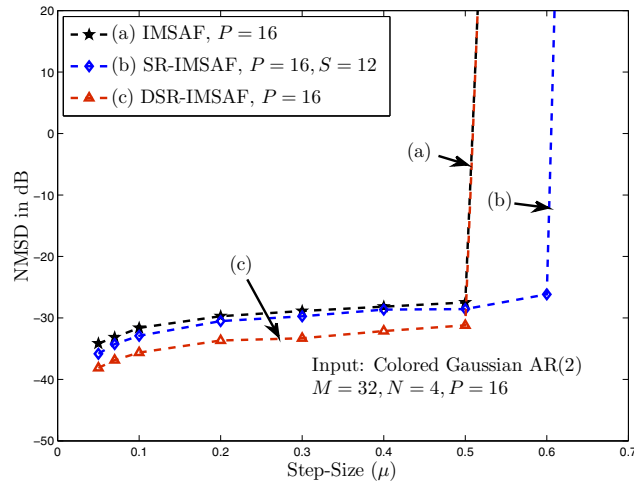


Fig. 34. The simulated steady-state NMSD values of IMSAF, SR-IMSAF, and DSR-IMSAF as a function of the step-size for $P = 16$ (Input signal: Colored Gaussian AR(2)).

Since $E\{\mathbf{v}_{i,D}(k)\mathbf{v}_{i,D}^T(k)\} = \sigma_{v_{i,D}}^2 \mathbf{I}$, we have

$$\sum_{i=0}^{N-1} E\{\mathbf{v}_{i,D}^T(k)[\mathbf{X}_i^T(k)\mathbf{X}_i(k)]^{-1}\mathbf{e}_{i,D}(k)\} = \sum_{i=0}^{N-1} \sigma_{v_{i,D}}^2 \text{Tr}(E\{[\mathbf{X}_i^T(k)\mathbf{X}_i(k)]^{-1}\}). \quad (75)$$

By substituting (75) into (71), Eq. 26 is established.

REFERENCES

- [1] B. Widrow and S. D. Stearns, *Adaptive Signal Processing*. Englewood Cliffs, NJ: Prentice-Hall, 1985.
- [2] S. Haykin, *Adaptive Filter Theory*. NJ: Prentice-Hall, 4th edition, 2002.
- [3] A. H. Sayed, *Adaptive Filters*. Wiley, 2008.
- [4] B. Farhang-Boroujeny, *Adaptive Filters: Theory and Applications*. Wiley, 1998.
- [5] K. Ozeki and T. Umeda, "An adaptive filtering algorithm using an orthogonal projection to an affine subspace and its properties," in *Electron. Commun. Jpn.*, vol. 67-A, 1984, pp. 19–27.
- [6] K. A. Lee and W. S. Gan, "Improving convergence of the NLMS algorithm using constrained subband updates," *IEEE Signal Processing Letters*, vol. 11, no. 9, pp. 736–739, Sep. 2004.
- [7] H. A. Doust and T. K. Shah, "NLMS algorithm with variable step-size using set-membership identification," *International Journal of Science and Technology, Scientia, Iranica*, vol. 9, pp. 378–384, Apr. 2002.
- [8] K. Dogancay, *Partial-Update Adaptive Signal Processing, Design Analysis and implementation*. Academic Press, 2009.
- [9] K. Y. Hwang and W. J. Song, "An affine projection adaptive filtering algorithm with selective regressors," *IEEE Trans. Circuits, Syst. II: EXPRESS BRIEFS*, vol. 54, no. 1, pp. 43–46, Jan. 2007.
- [10] S. J. Kong, K. Y. Hwang, and W. J. Song, "An affine projection algorithm with dynamic selection of input vectors," *IEEE Signal Processing Letters*, vol. 14, no. 8, pp. 529–532, Aug. 2007.
- [11] M. S. E. Abadi and V. Mehrdad, "Family of affine projection adaptive filters with selective partial updates and selective regressors," *IET Signal Processing*, vol. 4, pp. 567–575, 2010.
- [12] M. de Courville and P. Duhamel, "Adaptive filtering in subbands using a weighted criterion," *IEEE Trans. Signal Processing*, vol. 46, pp. 2359–2371, 1998.
- [13] J. J. Shynk, "Frequency domain and multirate adaptive filtering," *IEEE Signal Process. Mag.*, vol. 9, pp. 14–37, Jan. 1992.
- [14] M. S. E. Abadi and J. H. Husøy, "Selective partial update and set-membership subband adaptive filters," *Signal Processing*, vol. 88, pp. 2463–2471, 2008.
- [15] S. E. Kim, Y. S. Choi, M. K. Song, and W. J. Song, "A subband adaptive filtering algorithm employing dynamic selection of subband filters," *IEEE Signal Processing Letters*, vol. 17, no. 3, pp. 245–248, Mar. 2010.
- [16] M. K. Song, S. E. Kim, Y. S. Choi, and W. J. Song, "Selective normalized subband adaptive filter with subband extension," *IEEE Trans. Circuits, Syst. II: EXPRESS BRIEFS*, vol. 60, no. 2, pp. 101–105, Feb. 2013.
- [17] F. Yang, M. Wu, P. Ji, and J. Yang, "An improved multiband-structured subband adaptive filter algorithm," *IEEE Signal Processing Letters*, vol. 19, no. 10, pp. 647–650, Oct. 2012.
- [18] —, "Low-complexity implementation of the improved multiband-structured subband adaptive filter algorithm," *IEEE Trans. Signal Processing*, vol. 63, no. 19, pp. 5133–5148, Oct. 2015.
- [19] F. Yang, M. Wu, P. Ji, Z. Kuang, and J. Yang, "Transient and steady-state analyses of the improved multiband-structured subband adaptive filter algorithm," *IET Signal Processing*, vol. 9, pp. 596–604, 2015.
- [20] J. H. Husøy and M. S. E. Abadi, "Unified approach to adaptive filters and their performance," *IET Signal Processing*, vol. 2, pp. 97–109, 2008.
- [21] H.-C. Shin and A. H. Sayed, "Mean-square performance of a family of affine projection algorithms," *IEEE Trans. Signal Processing*, vol. 52, no. 1, pp. 90–102, Jan. 2004.
- [22] T. K. Moon and W. C. Sterling, *Mathematical Methods and Algorithms for Signal Processing*. Upper Saddle River: Prentice Hall, 2000.
- [23] K. Dogancay and O. Tanrikulu, "Adaptive filtering algorithms with selective partial updates," *IEEE Trans. Circuits, Syst. II: Analog and Digital Signal Processing*, vol. 48, pp. 762–769, 2001.
- [24] H. Malvar, *Signal Processing with Lapped Transforms*. Artech House, 1992.